博 士 論 文

The differences of collagen XVII between the oral mucosa and the skin discover the pathogenesis of oral lesions in pemphigoid

(17 型コラーゲンに着目した類天疱瘡における口腔内水疱形成機序の解明)

平成 31 年 3 月申請

北海道大学

大学院歯学研究科口腔医学専攻

鎌口真由美

The differences of collagen XVII between the oral mucosa and the skin discover the pathogenesis of oral lesions in pemphigoid

Mayumi Kamaguchi[1,2], Hiroaki Iwata[2], Hideyuki Ujiie[2], Ken Natsuga[2], Wataru Nishie[2], ,

Hiroshi Shimizu[2], Yoshimasa Kitagawa[1]

[1] Department of Oral Diagnosis and Medicine, Hokkaido University Graduate School of Dental Medicine

[2] Department of Dermatology, Hokkaido University Graduate School of Medicine

Running title: The pathogenesis of oral lesions in pemphigoid

Key words: keratinocyte, collagen XVII, oral mucosa, bullous pemphigoid, depletion

Word count: 8,408 words

Figures: 12 figures

Conflicts of interest: None to declare

Abbreviations

K: keratin, BMZ: basement membrane zone, COL17: collagen XVII, COL4: collagen IV, ECM: extracellular matrix, AISBDs: autoimmune subepidermal blistering diseases BP: bullous pemphigoid, MMP: mucous membrane pemphigoid, DIF: direct immunofluorescence, IIF: indirect immunofluorescence, ELISA: enzyme-linked immunosorbent Assay NC: noncollagenous, NHEK: normal human skin, NHOM: normal human oral mucosa, NHEKs: normal human epithelial keratinocytes, NHOMKs: normal human oral mucosal keratinocytes, YWHAZ: tyrosine 3-monooxygenase/tryptophan 5-monooxygenase activation protein zeta, GAPDH: glyceraldehyde 3-phosphate dehydrogenase, H&E: hematoxylin and eosin**,** mAb**:** antibody, HD & ECM: hemidesmosome and ECM fraction, BSA: bovine serum albumin BSA, TMB: tetramethylbenzidine, DMEM: Dulbecco's modified Eagle's medium, mIgG1: normal mouse IgG1, Dsgs: desmogleins,

Abstract

The basement membrane zone (BMZ) consists of multiple components, including collagen XVII (COL17), which is the major targeted antigen of pemphigoid diseases such as bullous pemphigoid (BP) and mucous membrane pemphigoid (MMP). The blistering mechanisms in pemphigoid have not been fully elucidated, especially in MMP, which mainly affects the mucosa. No research has addressed the differences in BMZ components between the skin and the oral mucosa. In this study, we investigate the differences of BMZ proteins especially COL17 between the skin and the oral mucosa to elucidate the pathogenesis of oral lesion in pemphigoid. We showed that the MMP sera react preferentially to the oral mucosal substrates than the skin substrates. As well as the diversity of the reactivity of MMP autoantibodies, it was suggested that there are certain differences between the skin and the oral mucosa as autoantigens itself. We found that the expression levels of COL17 were significantly higher in normal human oral mucosal keratinocytes (NHOMKs) than in normal human epidermal keratinocytes (NHEKs). The high expression levels of COL17 compensate for

COL17-depletion induced by pemphigoid IgG. These results may influence the clinical differences in pemphigoid. Furthermore, using immunoprecipitation, we revealed that COL17 directly binds to collagen IV (COL4) in NHEKs and NHOMKs. In particular, the C-terminus of COL17 is binding site to COL4 in NHOMKs. MMP-IgG or monoclonal antibody recognizing the C-terminus hindered the interaction of COL17 with COL4 in NHOMKs. These results are clinically relevant to less inflammatory phenotype in MMP. The inflammatory infiltrates around perilesions were significantly less in MMP compared to BP. These results indicate that pemphigoid IgG targeting the C-terminus plays a pathogenic role in blister formation in the oral mucosa to inhibit protein interactions with less inflammation.

Introduction

Both the skin and the oral mucosa have several important functions, such as providing a barrier, thermoregulation, sensation and immunity to maintain homeostasis of the body. However, distinct differences exist between the skin and the oral mucosa. Structurally, the skin has a keratinized epidermis, and hair follicles and sweat glands in the dermis. The oral mucosa has two types of epithelium: non-keratinized (soft palate, under-side of tongue, alveolar mucosa, labial mucosa, buccal mucosa) and keratinized (gingiva, hard palate). In the lamina propria, there are salivary glands. The non-keratinized epithelium has a structure somewhat different from that of the skin. [1]. Although keratin (K)5/14 are expressed in both types of basal cells, K4/13 are mainly expressed in the oral mucosa and K1/10 are mainly expressed in the skin [2]. Secretory IgA plays an important role in mucosal immunity [3]. Isolated oral keratinocytes demonstrate accelerated migration and greater proliferation than skin keratinocytes [2,4-6]. Although, the differences between the skin and the oral mucosa have been extensively addressed, no research has focused on the differences between these tissues in terms of their epithelial basement membrane zone (BMZ) components.

The BMZ can be differentiated by transmission electron microscopy into four major subregions [7]: 1) the plasma membrane of the basal keratinocytes, 2) the lamina lucida, 3) the lamina densa, and 4) the sublamina densa (Figure 1). Within the BMZ, multiprotein complexes called hemidesmosomes anchor keratinocytes to the underlying basement membrane [7-10]. Classic type I hemidesmosomes are found in the epidermis, and they consist of six major components: BP230, plectin, CD151, integrin α6, integrin β4, and collagen XVII (COL17, also called BP180) [10]. Laminin 332 and collagen IV (COL4) are extracellular matrix (ECM) proteins that are located in the lamina densa [11,12]. Collagen VII (COL7) , which is a major component of anchoring fibrils, is found under the lamina densa [13,14] (Figure 1). In hemidesmosome assembly, transmembrane COL17 interacts extracellularly with integrin α6 [15] and laminin 332 [16,17] and intracellularly with BP230 [18,19], plectin [18,20] and integrin β4 [15,19,21]. In the congenital skin blistering disease epidermolysis bullosa, these BMZ proteins are defective [22]. In addition, BMZ proteins are targeted by autoantibodies in several autoimmune subepidermal blistering diseases (AISBDs), such as COL17 for bullous pemphigoid (BP) and mucous membrane

pemphigoid (MMP), COL7 for epidermolysis bullosa acquisita, and laminin 332 and integrin α6β4 for MMP [23-27]. Among them, COL17 is targeted by both BP and MMP [23,24].

BP is the most common AISBDs, characterized by tense blisters accompanied by urticarial erythema on the skin (Figure 2a). Mucous membranes are also affected in 10-20% of patients. MMP is a rare autoimmune subepithelial blistering disease that predominantly affects the mucosal membranes (Figure 2b), but also affects the skin in some cases. In both diseases, histological analysis reveals junctional separation at the level of BMZ accompanied by inflammatory cell infiltration. Direct immunofluorescence (DIF) typically shows linear deposits of IgG and/or C3, along the BMZ. The deposits of IgA are sometimes observed in MMP. Indirect immunofluorescence (IIF) using normal human skin detects circulating autoantibodies in patients' sera (Figure 2). Although the histological and immunological findings are similar in BP and MMP, predominant involved organs differ between these two diseases. The diagnosis of BP and MMP is confirmed based on clinical findings and

laboratory examinations. Reaching a definitive diagnosis for MMP is often difficult because of the heterogeneous manifestations and inconclusive biopsies. Moreover, circulating autoantibodies are detected less frequently in MMP than in BP[28]. This has been attributed to the lower titers of the autoantibodies in MMP than in BP[29]. There are several immunological tests for detecting the autoantibodies of pemphigoid patients, including IIF, immunoblotting and Enzyme-Linked ImmunoSorbent Assay (ELISA).

COL17 is a type II-oriented 1,497-amino acid transmembrane protein. It contains 15 collagenous domains and 16 noncollagenous (NC) domains [30]. Differences in the major targeted epitopes on COL17 are reported in BP and MMP: the NC 16A domain in BP[31] and the C-terminus in MMP[32]. However, it remains unclear how autoantibodies targeting different epitopes induce diverse clinical manifestations. Moreover, no convincing evidence has explained why BP and MMP show the site specific manifestations.

We investigate the differences of BMZ proteins especially COL17 between the skin and

the oral mucosa to provide the possible reasons why predominant oral lesions occur in MMP but not in BP. For the clinical research, we firstly examined the reactivity of MMP and BP sera to the skin and the oral mucosal substrates[33]. Subsequently, we compared the expression levels of BMZ proteins between the skin keratinocytes and the oral mucosal keratinocytes using various methods including qPCR and immunoblotting[34]. Furthermore, we investigate the differences of COL17-interaction with other BMZ proteins especially COL4 to elucidate the blister mechanism of oral lesion in pemphigoid.

Materials and methods

BP or MMP patients and total IgG purification

We obtained sera from 20 BP and 20 MMP patients referred to the dermatology department and oral diagnosis and medicine department of Hokkaido University Hospital from April 2012 through March 2016. MMP patients fulfilled the following inclusion criteria; (i) clinical blistering or erosion on the oral mucosa, and (ii) linear

deposits of IgG and/or C3 at the BMZ by DIF. BP patients fulfilled the following inclusion criteria: (i) clinical blistering or erosion on the skin, (ii) linear deposits of IgG and/or C3 at the BMZ as determined by DIF, and (iii) circulating autoantibodies against COL17 as detected by COL17-NC16A ELISA/CLEIA (MBL, Nagoya, Japan). Non-NC16A BP patients fulfilled the following inclusion criteria (i) clinical blistering or erosion on the skin, and (ii) linear deposits of IgG and/or C3 at the BMZ by DIF., and iii) circulating autoantibodies detected by full-length COL17 ELISA [35], but not by COL17-NC16A ELISA/CLEIA (MBL, Nagoya, Japan). DIF, IIF, 1M NaCl split skin IIF, and COL17 ELISA were performed as previously described [35-37]. Total IgG was purified using a protein G affinity column according to the manufacturer's instructions (GE Healthcare, Amersham, UK) (final concentrations: 20mg/ml).

Mice

To generate the COL17-humanized mice, human COL17-transgenic mice (C57BL/6 background) expressing the squamous epithelium-specific K14 promoter and human *COL17* cDNA (m*Col17*$^{+/+}$, h*COL17*$^{+/+)}$ were crossed with heterozygous m*COl17*$^{+/-}$

mice (the F1 mouse had a 129/SvEvX C57BL/6 background, back-crossed with C57BL/6 over 10 generations)[38]. Neonate C57BL/6J mice were used to generate primary murine keratinocytes.

Production of recombinant COL17

Full-length human COL17 cDNA (NM-000292, Met^{1} to Pro^{1497}) was introduced into the Notl site of pcDNA5/FRT, designated as COL17 cDNA. To generate different deletion mutants, a 572-bp Xbal-digested fragment was first cut out, and the digested plasmid was self-ligated to obtain xbal-digested COL17 cDNA. Next, PCR reactions using forward primer Clal-F 5'-AGGGGTC*ATCGAT*GCTCTCACT-3' (the Clal digestion site is shown in italics) and different reverse primers, including COL17Δ1 5'-CGC*TCTAGA*T**CA**GTCAGTGCCATAGGGACCCC-3' (the Xbal digestion site is shown in italics and the stop codon in bold) to generate the $Met1$-Asp^{1340} amino acid fragment of collagen XVII designated as COL17Δ1, COL17Δ2 5'-CGCTCTAGATCATCTGAATTCAGACCCTCGCA-3' (the Xbal digestion site is

shown in italics and the stop codon in bold) for Met^{1} to Arg^{1174} amino acids designated as COL17Δ2 [17,39] (Figure 3).

Artificial split skin and mucosa using human tissues

Normal human skin (NHS) and normal human oral mucosa (NHOM) were obtained from uninvolved skin or mucosa of surgical specimens. To create artificial dermal-epidermal separations in skin and oral mucosa, the specimens were incubated with 1 M NaCl for 24 hours at 4°C [37], or 5 mM EDTA for 6 hours in the skin or 8 hours in the oral mucosa at 4°C [40].

Cell culture

Primary normal human epithelial keratinocytes (NHEKs) normal human oral mucosal keratinocytes (NHOMKs) were generated from uninvolved skin or mucosa of surgical specimens or normal healthy volunteers. Murine skin and oral mucosal keratinocytes were generated from neonate C57BL/6J mice, mixed from more than five neonate mice. Each specimen was placed in dispase (1,000 PU/ml, Wako, Osaka, Japan) overnight at

4°C, and the epidermis was separated from the dermis. After incubation in trypsin (0.05 w/v% trypsin-0.53 mM/EDTA/4Na, Wako, Osaka, Japan) for 7 minutes at 37°C, the cell suspension was filtered through a 40-μm cell strainer (Thermo Fisher Scientific, Rockford, IL) followed by centrifuging at 270 G for 3 minutes at 20°C. After the supernatant was aspirated, the pellet was resuspended in keratinocyte growth medium (KGM-Gold, Lonza, Basel, Switzerland) and cultured at 37 °C under 5% CO_2. NHEKs were purchased for the control (Lot number: 0000399827, Lonza, Basel, Switzerland). For the NHEKs and NHOMKs, no more than four passages were used in this study.

Quantitative RT-PCR

The expression of *hCOL17A1, hLAMC2, hCOL7A1, hITGA6, hITGB4, hKRT1, hKRT13, mCol17a1, mLamc2, mCol7a1, mItga6, mItgb4, mKrt1,* and *mKrt13* was measured by the cycle threshold (ΔΔ*CT*) method using each primer set (Table 1). mRNA was extracted from NHEKs and NHOMKs, mouse keratinocytes established from tail skin or buccal mucosa in C57BL/6J mice, and mouse tissues from tail skin and buccal mucosa by using the RNeasy Mini Kit (Qiagen, Valencia, CA). Single-stranded cDNA

was synthesized using the RT2 First Strand Kit (Qiagen, Valencia, CA). According to the manufacturer's instructions, assays were performed using RT^2 SYBR GREEN/ROX PCR Master Mix (Qiagen, Valencia, CA) and Step-OnePlus (Applied Biosystems). Relative expression ratios were normalized to tyrosine 3-monooxygenase/tryptophan 5-monooxygenase activation protein zeta (YWHAZ), or glyceraldehyde 3-phosphate dehydrogenase (GAPDH).

Hematoxylin and eosin (H&E) staining

NHS and NHOM were frozen, and 5-μm-thick sections were prepared by cryostat (Leica Biosystems, Tokyo, Japan). Sections were used for H&E and immunofluorescent stainings as descried below. For H&E staining, the specimens were fixed by 79% / v 99.5% ethanol, 20% / v formalin (Mildform 10N, Wako, Osaka, Japan) and 1%/v acetic acid (Wako, Osaka, Japan) for 2 minutes at room temperature. After washing with PBS, the nuclei were stained with Mayers hematoxylin (Muto, Tokyo, Japan) for 3 minutes. After rinsing in distilled water, the specimens were stained with 1% eosin Y (Wako, Osaka, Japan) for 1 minute, followed by dehydrate by 99.5% ethanol.

Immunofluorescent staining

For IIF, Specimens were stained with patient's sera (1:20 dilution in PBS) as primary antibodies for 45 minutes at 37°C, followed by incubation with FITC-conjugated anti-human IgG (1:100, DakoCytomation, Glostrup, Denmark) as secondary antibodies for 45 minutes at 37°C. We tested two individual substrates for each sera and defined positivity as the presence of autoantibodies in at least in one the substrates.

Skin, oral mucosa, tongue, and esophageal specimens were obtained from the COL17-humanized mice ($mCOL17^{-/-}$, $hCOL17^{+/+}$). Given the low homology between human and mouse COL17, we used COL17-humanized mice instead of wild-type mice. These organ samples were used as substrates for the IIF test.

For immunofluorescent staining of BMZ proteins, specimens were stained with anti-human COL17 monoclonal antibody (mAb) targeting COL17-NC16A (TS39-3[41], final concentration 2 μg/ml), human laminin 332 (laminin 5, 1:100, Abcam, Cambridge, UK), anti-human COL7 (LH7.2, 1:100, Abcam, Cambridge, UK), anti-human integrin α6 mAb (GoH3, 1:100, Abcam, Cambridge, UK) and anti-human integrin β4 (3E1,

1:100, Abcam, Cambridge, UK) as primary antibodies for 45 minutes at 37°C. Specimens were then incubated with FITC-conjugated anti-mouse, anti-rabbit or anti-rat IgG (DakoCytomation, Glostrup, Denmark) as secondary antibodies for 45 minutes at 37°C. The nuclei were stained with propidium iodide (Life Technologies, Tokyo, Japan). Observations were carried out by fluorescence microscopy (Olympus, Tokyo, Japan) and confocal laser scanning microscopy (Olympus, Tokyo, Japan).

Immunoblotting

NHEKs and NHOMKs were lysed with RIPA buffer (Thermo Fisher Scientific, Rockford, IL) containing protease inhibitor cocktails (Sigma Aldrich, St. Louis, MO). For immunoblotting, we prepared hemidesmosome and ECM fraction (HD & ECM), in which the enriched hemidesmosomal proteins and ECM proteins remained[42]. Briefly, NHEKs and NHOMKs were cultured to approximately 80-90% confluence in keratinocyte growth medium (KGM-Gold, Lonza, Basel, Switzerland) for 24 hours. After washing with PBS, the cells were incubated with 20 mM NH_4OH for 5 minutes at room temperature. After all the cells had detached, the HD & ECM was treated with

0.1% Triton X-100 (Sigma Aldrich, St Louis, MO) in PBS for 5 minutes to solubilize and remove membranous debris. Then, the HD & ECM was extensively washed with PBS and dissolved in SDS-PAGE sample buffer. The protein concentration of the sample was measured using the BCA Protein Assay Kit (Thermo Fisher Scientific, Rockford, IL) due to lack of appropriate loading controls. Samples were applied to 6% SDS-polyacrylamide gel for SDS-PAGE with equal amount of total protein (3 μg/lane).

In some experiments, immunoblotting with Triton X-100-soluble or -insoluble fractions was used [43]. Cells were lysed in 1% Triton X-100 (Sigma Aldrich, St Louis, MO) in PBS containing a protease inhibitor cocktail (Sigma Aldrich, St Louis, MO), followed by centrifugation. The resultant supernatant was used as the cytosol/membrane fraction. Triton X-100-insoluble pellets were solubilized in 2% SDS sample buffer and stored as the cytoskeleton fraction, containing hemidesmosomal components.

For the immunoblotting, the gels were transferred to a nitrocellulose membrane (Bio-Rad Laboratories, Hercules, CA). After blocking for 1 hour at room temperature in 2% skimmed milk in TBS/T, the membranes were incubated with 1:500 diluted anti-human COL17 (09040, final concentration 2 μg/ml) [41], anti-human laminin γ2

(D4B5, 1:500, EMD Millipore, Burlington, MD), anti-human COL7 (LH7.2, 1:100, Abcam, Cambridge, UK), anti-human integrin α6 (ITGA6, 1:500, Sigma-Aldrich, St. Louis, MO) or anti-human integrin β4 (sc-9090, 1:500, Santa Cruz Biotechnology, Dallas, TX), anti-human COL4α1 Ab (Collagen IV alpha 1, 1:500, Novos Biologicals, Littleton, CO)with 2% skimmed milk in TBS/T overnight at 4°C. HRP-conjugated or anti-mouse or anti-rabbit IgG (1:5,000 dilution, Life Technologies, Carlsbad, CA) in TBS/T was reacted for 1 hour at room temperature. Signals were visualized with Clarity Western ECL Substrate (Bio-Rad Laboratories, Hercules, CA).

Immunoprecipitation

NHEKs and NHOMKs were lysed with 1% octylphenoxypolyetheanol (Nonidet P-40, Caledon Laboratories Ltd, Georgetown, Canada), containing protease inhibitor cocktails (Sigma Aldrich, St. Louis, MO). TS39-3, anti-human COL17 mAb targeting the C-terminus of COL17 (C17-C1)[44], anti-DDDDK mAb (M2, Sigma Aldrich, St Louis, MO), anti-human COL4α1 Ab (PHM-12+CIV22) or mIgG1 (Sigma Aldrich, St. Louis, MO) (10 μg) was diluted in 200 μl of PBS and then incubated with 25 μl protein G

coupled Dynabeas (Thermo Fisher Scientific, Rockford, IL) for 1 hour at room temperature. Then, 100 µl cell lysates were diluted in 400 µl of PBS and incubated with Dynabease-Ab complex over night at 4°C. After washing with PBS, sample were boiled for 5 minutes at 95°C.

***In vitro* binding test between COL17 and COL4**

The 96 well plates (Thermo Fisher Scientific, Rockford, IL) were coated with 500 ng/well of human COL4 protein (Sigma Aldrich, St. Louis, MO) in 50 mM carbonate buffer pH 9.5 over night at 4°C. Non-specific binding was reduced by blocking plates with 2% bovine serum albumin (BSA) in PBS for 1 hour at room temperature. Human COL17 recombinant proteins were added at 500 ng/well and incubated for 2 hours. To quantify COL17 binding to COL4, full-length human COL17 recombinant protein was used with serial dilutions, and the standard curve was generated. After extensive washing, the plates were incubated with HRP conjugated anti-DDDDK mAb (M2, 1:20,000, Sigma Aldrich, St. Louis, MO). After another washing, the enzyme substrate solution containing 3, 3', 5, 5'-tetramethylbenzidine (TMB) was added to each well.

The enzyme reaction was allowed to proceed for 20 minutes in the dark, at which point the color reaction was stopped by adding 0.12 N hydrochloric acid (HCl). The absorbance was measured at 450 nm with the correlation wavelength set at 620 nm by a microplate reader (TECAN Austria GmbH). To evaluate the binding disturbance between COL17 and COL4, COL17 recombinant proteins (250 ng/well) were preincubated with mAbs TS39-3 or C17-C1 (250 ng/well), MMP-IgG or BP-IgG (20 μg/well) for 1 hour at room temperature and then added to the plates. To quantify COL17 binding to COL4, full-length human COL17 recombinant protein was used with serial dilutions, and the standard curve was generated. After blocking with 2% BSA in PBS for 1 hours at room temperature, the plates were incubated with HRP conjugated anti-DDDDK mAb (M2, 1:20,000, Sigma Aldrich, St. Louis, MO). The enzyme reaction was allowed to proceed for 20 minutes. The absorbance was measured at 450 nm with the correlation wavelength set at 620 nm by a microplate reader (TECAN Austria GmbH).

Competitive COL17-ELISA

To investigate whether MMP-IgG had an identical epitope with mAb C17-C1, we performed competitive COL17-ELISA. The 96 well plates (Thermo Fisher Scientific, Rockford, IL) were coated with 250 ng/well of human full-length COL17 in 50 mM carbonate buffer pH 9.5 over night at 4°C. After blocking with 2% BSA in PBS, the plates were incubated with MMP-IgG, BP-IgG, or normal human IgG (20 μg/well) for 1 hours. After extensive washing, mAbs TS39-3 or C17-C1 (40 ng/well) was incubated, followed by HRP-conjugated anti-mouse IgG (1:20,000, Sigma Aldrich, St. Louis, MO). The enzyme reaction was allowed to proceed for 20 minutes. The absorbance was measured at 450 nm with the correlation wavelength set at 620 nm by a microplate reader (TECAN Austria GmbH).

Treatment of cultured keratinocytes with mAbs against COL17

To investigate COL17 depletion, NHEKs and NHOMKs were treated with mAbs. NHEKs and MHOMKs were cultured to approximately 60% to 70% confluence for 24 hours in CnT-Prime (CELLnTEC, Bern Switzerland). Cells were treated with mAb TS39-3 targeting the NC16A domain of human COL17 [41] and/or C17-C1 targeting the

C-terminus of human COL17 [44] (total concentration: 2.5 μg/ml) for 4 hours, and then lysed with RIPA buffer (Thermo Fisher Scientific, Rockford, IL) containing protease inhibitor cocktails (Sigma Aldrich, St. Louis, MO).

Cell adhesion test

NHEKs and NHOMKs were seeded in 12-well plates and cultured. The culture plates were placed on the vortex for 20 minutes for vibration. The numbers of cells remaining were counted as the number of NHEKs and NHOMKs adhered to the bottom of the plate. As a control, NHEKs and NHOMKs were cultured without vortex stimuli. Cells retained on the bottom of the culture plate were treated with 0.25% trypsin (Wako, Osaka, Japan) for 5 minutes at 37°C and released completely into the medium by pipetting. The released cells were counted using a blood cell counter under a microscope.

For the cell adhesion test of NHKs or NHOMKs under COL17 knockdown, we used RNA interference approaches to knock down COL17 expression in the keratinocytes. Briefly, 12 pM of siRNA or the control (Mock) (Silencer Select siRNAs, Thermo Fisher,

Waltham, Massachusetts, USA) was diluted with 200 μl optiMEM (Thermo Fisher Scientific, Rockford, IL), and then 2 μl of Lipofectamin®RNAiMAX (Thermo Fisher Scientific, Rockford, IL), was incubated in 6-well plates for 20 minutes at room temperature. NHEKs and NHOMKs (2×10^5/well) were added and incubated for 48 hours at 37°C and used for the cell detachment assay. Total RNA and protein were harvested and analyzed by RT-PCR and immunoblotting to confirm efficacy.

Cell adhesion test to COL4 coated plate

12-well plates were coated with human COL4 (Cell matrix type IV collagen, NITTA, Osaka, Japan) with 1 mM of HCl. NHOMKs were seeded in plates and cultured in CnT-Prime (CELLnTEC, Bern Switzerland) for 24 hours. The medium was changed to Dulbecco's modified Eagle's medium (DMEM) (Life Technologies, Tokyo, Japan), containing 1.8 mM of calcium simultaneously with mAb C17-C1 or mIgG1 (2.5 μg/ml) and cultured for 12 hours. After vibration stress, the remaining cells on the plates were counted.

Statistical analysis

Graph Pad PRISM software version 7.0 was used to analyze the quantitative data. P-values were determined using Student *t*-test or one-way ANOVA followed by Tukey's test. A value of $P<0.05$ was considered statistically significant. $*P<0.05$; $**P<0.01$; $***P<0.001$. Experiments were performed at least three times.

Ethics Statement

All studies conformed to the guidelines of the medical ethics committee of Hokkaido University and the Declaration of Helsinki Principles. Written informed consent was obtained before any samples were collected. A full review and approval by an ethics committee of Hokkaido University were not required, according to local guidelines. The studies were conducted in accordance with the Helsinki guidelines.

Results

1. BP and MMP autoantibodies react differently to the skin and the oral mucosa

1) The oral mucosa is more sensitive than the skin for detecting MMP autoantibodies

The results of each patient from MMP and BP are shown in Table 2. IIF using NHS demonstrated linear staining for IgG in 7 (35%) of the MMP sera in this study (Table 3). In contrast, IIF using NHOM as a substrate detected 17 cases (85%). The positive rate was higher than that of IIF using NHS (Table 2,3p=0.0036). Although staining intensity was weak, IgG deposits of several MMP sera were clearly detected in mucosal but not skin substrates (Figure 4a). All of the BP sera reacted to the skin substrates, but 18 (90%) of sera showed positive staining at the BMZ in the mucosal substrate (Table2,3. Figure 4a). The overall results are shown in Table 2.

2) Antibodies targeting the C-terminus of COL17 preferentially reacted to mucosal BMZ

The reactivity of autoantibodies from MMP were different in skin and mucosal substrates. Next, we tested the reactivity of two different mAbs targeting different epitopes of human COL17. mAbs (TS39-3/C17-C1) showed distinct reactivity to skin

and oral mucosa. The mAb TS39-3, targeting human COL17-NC16A, and the mAb C17-C1, targeting the C-terminus of human COL17, reacted to the BMZ at the same intensity on the skin, as described in a previous report[44] (Figure 4,b). In contrast, the mAb TS39-3 showed less reactivity than the mAb C17-C1 against the BMZ on oral mucosa (Figure 4,b).

3) MMP sera showed diverse reactivity to different organs

Like as mucosal and skin substrates, the reactivity of autoantibodies might be diverse in different mucosal substrates, such as buccal mucosa, tongue or esophagus. Because it is hard to get various human organ samples for the comparison of serum reactivity, we performed the IIF on the several organ samples obtained from COL17-humanized mice to compare the differences in reactivity of MMP sera for each organ.

Of the MMP cases, 10 (50%) sera showed positive reactivity against BMZ in the buccal mucosa of COL17-humanized mice, whereas 7 sera (35%) were positive with skin. 4 sera (20%) and 8 sera (40%) were positive with the tongue and esophagus, respectively (Table 3). In contrast, BP sera reacted to all organ samples. Representative figures are

shown in Figure 4c.

4) Autoantigens of MMP were identified by immunoblotting using NHOMK lysate.

IgG reactivity to a 180-kDa protein corresponding to COL17 was found in 2 (10%) of MMP sera on immunoblotting using NHEK lysate (Table 3). In contrast, 11 (55%) of MMP IgG reacted to COL17 on immunoblotting with NHOMK lysate (Table 3, p=0.0012, Figure 4d). The results for each patient are shown in Table 2. One serum reacting to the dermal side in 1M NaCl-split skin IIF was diagnosed as laminin332-type MMP using purified protein of laminin332[23]. As for BP, IgG reactivity to COL17 was found in 19 (95%) of BP sera on both NHEKs and NHOMKs extract. (Table3, Figure 4e). The results for each patient are shown in Table 2.

2. High expression of COL17 in the oral mucosa compemsate its depletion induced by pemphigoid IgG

1) COL17 stains more brightly in the BMZ of the oral mucosal epithelia than in the skin

Besides the differences of reactivities in autoantibodies to the skin and the oral mucosa, antigen itself was expected to be attribute to the distinct clinical manifestations between BP and MMP. Therefore, we explore the differences of BMZ proteins between the skin and the oral mucosa. We started to investigate the staining pattern of several BMZ proteins, including COL17, laminin 332, COL7 and integrin α6β4, which are targeted by autoantibodies of AISBD, using NHS and NHOM (n=3). Histologically, the epithelium is thicker in the oral mucosa than in the skin, as previously reported [45] (Figure 5a). COL17 is distributed in the bottom and the lateral-apical sides of basal keratinocytes in the skin [46-48]. COL17 was clearly detected in the bottom and in the lateral-apical sides of the oral mucosa cells, just as it was detected there in the skin cells. However, COL17 is brighter in the oral mucosa BMZ than in the skin BMZ. Integrin α6β4 stained slightly in the apical-lateral regions of the skin and the oral mucosa. Laminin 332 and COL7 stained only at the BMZ in both the skin and the mucosa (Figure 5a).

2) Artificial splits in the oral mucosa were not along the lamina lucida

IIF using 1 M NaCl-split skin is useful to differentiate AISBD autoantibodies from lamina densa- and sublamina densa-targeted ones [37]. The separation in 1 M NaCl-split skin runs along the intralamina lucida, which suggests a weakness in the lamina lucida [49]. We introduced artificial splits in NHS and NHOM treated with 1 M NaCl or 5 mM EDTA (n=3). Histologically, the separation was less clear in the NHOM than in the NHS. Basal keratinocytes were detected on both sides of split in the NHOM (Figure 5b, upper panel). COL17 stained on the epidermal side of the split in the NHS treated with 1 M NaCl or 5 mM EDTA (Figure 5b, left panels), which is consistent with a previous report [49]. Unexpectedly, COL17 stained on both the epithelial and the subepithelial sides of the split in NHOM treated with 1 M NaCl or 5 mM EDTA (Figure 5b, right panels). Furthermore, it took longer for the separation to occur in NHOM than in NHS by treatment with EDTA. These results suggest that the basal keratinocytes in the oral mucosa show stronger adhesion to the basement membrane than do the basal keratinocytes of the skin.

3) *COL17A1* expression is significantly higher in normal human oral mucosal

keratinocytes than in normal human epidermal keratinocytes

Immunofluorescence is proposed to be limited to detect the precise protein levels existing in human tissues. To prove the results of immunofluorescent staining, we compared the mRNA and protein expression levels using cultured keratinocytes or murine tissues. We generated NHOMKs from healthy individuals. We first examined the expression of those keratins that are useful differentiation markers of the skin and oral mucosa [2]. *KRT1* expression was higher in NHEKs than in the NHOMKs, whereas *KRT13* expression was higher in the NHOMKs than in the NHEKs ($p<0.0001$, $p=0.0344$, Figure 6a).

To explore the quantitative differences in the BMZ proteins (COL17, laminin 332, COL7, integrin α6β4), we compared the mRNA levels using keratinocytes (n=3, Figure 6a). Laminins are heterotrimer proteins that consist of α, β, and γ-chains. It is known that laminin 332, laminin 311, laminin 511, and possibly laminin 321 are present in the epidermal basement membrane [50]. Because γ2 is a unique chain to compose laminin 332, we selected laminin γ2 to analyze the laminin 332. *COL17A1* expression was 50% higher in the NHOMKs than in the NHEKs ($p=0.0033$). *LAMC2* and *COL7A1*

expression levels were also higher in the NHOMKs than in the NHEKs (*LAMC2*: p=0.0258, *COL7A1*: p=0.0167). There were no significant differences for *ITGA6* and *ITGB4*.

To exclude the possibility of the contribution of interindividual variation to the differences, we subsequently investigated the mRNA levels using keratinocytes obtained from a single individual (n=1). Keratinocytes were established using both skin and oral mucosa samples from a healthy 33-year-old woman. Just as with the results for different persons, the *COL17A1* and *COL7A1* expression levels for a single individual were higher in the NHOMKs than in the NHEKs (*COL17A1*: p=0.0251, *COL7A1*: p=0.0097) (Figure 7a). Although the *LAMC2* expression level was slightly higher in the NHOMKs in the interindividual data, there were no significant differences. The sample number of analysis using single individual is a disadvantage in this study. It is difficult to obtain both skin and the oral mucosa samples from a single individual, so we attempted to analyze the murine tissues and keratinocytes.

4) NHOMKs produced greater amounts of COL17 than did NHEKs

Next, to evaluate the protein expression, we performed immunoblotting to detect the BMZ components (COL17, laminin 332, COL7, integrin α6β4) using total cell lysate or HD & ECM. It is reported that the enriched hemidesmosomal proteins and ECM proteins remained after cells are removed by NH_4OH [42]. We compared these protein expressions between NHEKs and NHOMKs. Regarding total cell lysate, COL17 and laminin 332 had significantly higher expression in NHOMKs than in NHEKs (n=3, COL17: p=0.0254, laminin 332: p=0.0178, calculated band is 105 kDa laminin γ2, Figure 6b). In line with these results, the amounts of COL17 and laminin 332 were greater in NHOMKs than in NHEKs from a single individual. (n=1, COL17: p=0.0002, laminin 332: p=0.0281, Figure 4b). With regard to HD & ECM, COL17, laminin 332 and integrin α6 had significantly higher expression in NHOMKs than in NHEKs (n=3, COL17: p=0.0043, laminin 332: p=0.0267, integrin α6: p=0.0023, Figure 6c). The amounts of COL17, laminin 332 and integrin β4 were significantly greater in NHOMKs than in NHEKs from a single individual (n=1, COL17: p=0.0097, laminin 332: p=0.0185, integrin β4: p=0.0089, Figure 7c). The results of cell lysates and HD & ECM

found the amount of COL17 to be considerably greater in NHOMKs than in NHEKs.

5) *mCol17a1* expression is higher in murine oral mucosa than in murine skin

The mRNA was extracted from murine tissues and keratinocytes (tail skin and buccal mucosa). *mCol17a, mLamc2,* and *mCol7a1* have higher expression in the murine oral mucosa than in the murine skin (n=5, *Col17a*: $p<0.0001$, *mLamc2:* $p=0.0005$, *mCol7a1:* $p=0.0021$, Figure 8). Just as with the human results, *mCol17a, mLamc2,* and *mCol7a1* expression levels were higher in the murine mucosal keratinocytes than in the murine skin keratinocytes (n=4, *Col17a*: $p<0.0001$, *mLamc2:* $p<0.0001$, *mCol7a1:* $p=0.029$, Figure 8).

6) Cell adhesion strength is significantly higher for NHOMKs than for NHEKs

COL17 exists in both hemidesmosomes and nonhemidesmosomes in the skin [46-48]. Our immunofluorescent staining of COL17 clearly demonstrated lateral-apical staining not only in the skin but also in the oral mucosa. To evaluate the amount of COL17 consisting in hemidesmosomes and in nonhemidesmosomes individually, we prepared

Triton X-100-insoluble or -soluble fractions of NHOMKs and NHEKs. Triton X-100-insoluble fraction represents hemidesmosomal COL17, whereas Triton X-100-soluble fraction represents nonhemmidesmosomal COL17. For both fractions, the amount of COL17 was markedly greater in the NHOMKs than in the NHEKs (n=3, soluble: p=0.0148, insoluble: p=0.0033, Figure 9a). Because COL17 is apparently involved in cell adhesion, these results led us to test the cell adhesion strength by counting the cells remaining after vibration stress. The counts of remaining cells were significantly greater for NHOMKs than for NHEKs, which indicates that the NHOMKs adhered to the culture plates more strongly than did the NHEKs (n=3, p=0.028, Figure 9b). Next, we assessed the correlation of cell adhesion strength with COL17 expression levels using COL17-knockdown keratinocytes. The number of cells remaining was much lower with COL17 knockdown by siRNAs than without such knockdown (n=3, Figure 9c). The cell adhesion and knockdown experiments were reproducible in the keratinocytes from a single individual (n=1, Figure 10). The knockdown efficiencies were measured by qPCR and immunoblotting, and were found to exceed 80％ (Figure 9c). These results indicate that differential COL17 expression accounts for the

differences in cell adhesion properties between NHEKs and NHOMKs.

7) Anti-COL17 antibodies induce significantly greater COL17-depletion in NHEKs than in NHOMKs

Finally, to explain the clinical diversity of the predominant lesions in pemphigoid, we examined the COL17 depletion of NHEKs and NHOMKs treated with anti-COL17 IgG [51]. The C-terminus of COL17 is thought to be a major epitope of MMP, whereas the NC16A domain of COL17 is known as a pathogenic epitope for BP [23,32]. We treated the keratinocytes with mAbs targeting the NC16A domain (TS39-3) [41] and/or the C-terminus (C17-C1) [44]. Under treatment with mAb TS39-3, the amount of COL17 was reduced in the NHEKs and the NHOMKs in a dose-dependent manner (n=3, Figure 11a); however, much more COL17 remained in the NHOMKs than in the NHEKs (n=5, Figure 11b). This may be due to the great amounts of COL17 in NHOMKs under normal conditions (Figure 6 and 7). No reduction was seen for either cell type under treatment with mAb C17-C1. Interestingly, when keratinocytes were treated with mAbs TS39-3 and C17-C1 in combination, COL17 depletion was remarkably enhanced. mAb

C17-C1 caused additive shortages of COL17 in NHEKs and NHOMKs. We examined the cell adhesion strength of NHEKs and NHOMKs with mAbs TS39-3 and/or C17-C1. The cell adhesion strengths of both cells underwent a dose-dependent decrease with mAb TS39-3 alone or together with mAb C17-C1 (n=3, Figure 11c). These results indicate the possible pathogenicity of non-NC16A IgG.

3. The direct binding of COL17 and COL4 is disrupted by pemphigoid autoantibodies

1) Oral lesions in MMP are less inflammatory than skin lesion in BP

First, we evaluated the histopathological findings at lesional areas in BP and MMP. Patient information is summarized in Table 4. MMP showed significantly fewer inflammatory cell infiltrations, including eosinophils, compared to BP (Figure 12a, b). These findings indicated that the blisters occur with less inflammation in MMP.

2) **mAb targeting C-terminus (C17-C1) did not co-precipitate COL4**

Next, we investigated the interaction of COL17 with COL4. We precipitated COL17 and COL4 in cell lysates of NHEKs and NHOMKs by two mAbs targeting human COL17, mAb C17-C1 and mAb TS39-3 (Figure 3). mAbs TS39-3 and C17-C1 co-precipitated COL4 with COL17 in NHEK lysates (Figure 13a). In NHOMK lysates, COL17 and COL4 were clearly detected with precipitation using mAb TS39-3 (Figure 13b). However, when NHOMK cell lysate was incubated with mAb C17-C1, COL4 was not detected (Figure 13b). The anti-COL4 antibody co-precipitated COL17 in both NHEK and NHOMK lysates (Figure 13a, b). Both laminin 332 and integrin α6/β4 were detected when mAbs TS39-3 or C17-C1 were used for the precipitation (Figure 12c). These results indicated that COL17 directly interacts with COL4. However, the binding region of COL17 and COL4 may differ between NHEKs and NHOMKs and be hindered by mAb C17-C1 in NHOMKs.

3) **C-terminus of COL17 directly binds to COL4**

C-terminus of COL17 may bind to COL4 in the oral mucosa. To identify the precise binding region of COL17, we used HEK293 cells stably expressing full-length COL17

or the deletion mutants COL17Δ1 and COL17Δ2 [17]. The Met^{1} to Asp^{1340} amino acid fragment and the Met^{1} to Arg^{1174} amino acid fragment of COL17 were designated COL3 and NC6, respectively (Figure 3). Full-length COL17, COL17Δ1 and COL17Δ2 were precipitated with anti-DDDDK mAb (Figure 14a). In contrast, the amount of COL4 precipitated with anti-DDDDK mAb decreased with COL17Δ1 and COL17Δ2. COL17Δ2 was precipitated by mAb TS39-3 but not by mAb C17-C1 due to the epitope of mAb C17-C1 [44] (Figure 14a). COL4 was clearly detected when full-length COL17 and COL17Δ1 were precipitated with mAbs TS39-3 or C17-C1 (Figure 14a). However, COL4 was faintly detected when COL17Δ2 was precipitated with mAbs TS39-3 or C17-C1. These results suggested that amino acids Gly^{1175} to Asp^{1340} of COL17 mainly bound to COL4. To confirm these findings, we performed *in vitro* protein-protein binding assays. The amount of COL17Δ2 binding to COL4 was significantly reduced by approximately 90% (Figure 14b, $p<0.0001$), suggesting the direct binding of COL4 and COL17, particularly between Gly^{1175} to Asp^{1340} of COL17.

4) **Autoantibodies targeting the C-terminus of COL17 disrupt the binding**

between COL17 and COL4

The present data indicate that the binding region of COL17 with COL4 contains the epitope of mAb C17-C1. We performed *in vitro* protein-protein binding assays in the presence of mAbs TS39-3, C17-C1 and normal mouse IgG1 (mIgG1). When full-length COL17 was preincubated with mAb TS39-3 or mIgG1, the amount of COL17 binding to COL4 was unchanged (Figure 15a). In contrast, preincubation with mAb C17-C1 significantly reduced the amount of COL17 binding to COL4 by 70% (Figure 15a). The disturbing effects of mAb C17-C1 on COL17-COL4 binding were dose-dependent (Figure 15b). Next, MMP-IgG or BP-IgG (Table 5) was preincubated with COL17 before adding onto the COL4-coated plates. The amounts of COL17 binding to COL4 were significantly decreased when the COL4-coated plates were incubated with MMP-IgG (Figure 15c). In contrast, typical BP-IgG (NC16A) did not show significant inhibition of COL17-COL4 binding. Even non-NC16A BP-IgG did not prevent the binding of COL17-COL4 (Figure 15c). These results demonstrated that MMP-IgG hinders the binding of COL17 with COL4, similar to mAb C17-C1. On the other hand, the preincubation with MMP-IgG inhibited the binding of mAb C17-C1 to the ELISA

plates (Figure 15d, left). Furthermore, typical BP-IgG significantly prevented the binding of mAb C17-C1 and mAb TS39-3 (Figure 15d, left and middle). BP patients had polyclonal autoantibodies against not only NC16A but also regions outside of NC16A due to epitope spreading. None of the mIgG1 bound to COL17 (Figure 15d, right).

5) Antibodies targeting C-terminus of COL17 reduce the cell adhesion strength through the disruption of COL17-COL4 bindings

Finally, we investigated whether antibodies recognizing the C-terminus of COL17 reduced the cell adhesion strength. When the plates were coated with purified human COL4, the remaining cell counts after vibration stress were significantly higher compared to COL4-uncoated conditions (Figure 15e). In contrast, when mAb C17-C1 was added to the COL4-coated plates, the cell counts were significantly decreased (Figure 15f). IgG against NC16A, but not IgG against the C-terminus, induces COL17 depletion and reduces the cell adhesion strength in cultured keratinocytes [41,44,51,52]. In line with these findings, we tested COL17 depletion after mAb C17-C1 incubation in

NHOMKs for 12 hours. Although mAb TS39-3 induced COL17 depletion, neither mAb C17-C1 nor mIgG1 changed the amount of COL17 after the 12-hour treatment (Figure 15g).

Discussion

It is known that the pathogenic autoantibodies are crucial for generating autoimmune blistering diseases. As for the skin lesions in pemphigoid, various studies have revealed the pathogenic mechanism using experimental mice models and cultured keratinocytes However, the limited number of studies have focused on the pathogenicity of oral lesions in pemphigoid. We believe that the differences of the BMZ proteins between the skin and the oral mucosa may be the breakthrough to uncover the pathogenesis of oral lesions in pemphigoid.

Firstly, we noticed that the detection of autoantibodies in MMP patients is often difficult in account of the low titers of circulating autoantibodies. Although MMP predominantly affects the mucous membranes rather than the skin, conventional IIF

tests are usually performed using normal skin. We evaluated the different sensitivities of BP and MMP autoantibodies to the skin and oral mucosa. We revealed that the oral mucosal specimens or oral mucosal keratinocyte is useful substrate for detecting autoantibodies and identifying autoantigens in MMP. The reasons why the oral mucosal substrates detect MMP autoantibodies and autoantigens more sensitively than the skin substrates are not fully understood. We expected the two major factors to be responsible. One is autoantibodies, and the other is autoantigens. It is well known that the major epitopes on COL17 differ between MMP and BP. The C-terminus of COL17 is thought to be a major epitope of MMP[7], whereas the NC16A domain of COL17 is known as a pathogenic epitope for BP[41]. The epitope differences are associated with cellular responses. COL17-NC16A IgG, but not IgG against other epitopes on COL17, depletes keratinocytes of COL17[44,51-54]. This is thought to be one of the pathogenic mechanisms of COL17-NC16A IgG[55], while the pathogenicity of autoantibodies to C-terminus remains unknown. This epitope diversity of autoantibodies between MMP and BP may be associated with the reactivity to the skin and the oral mucosa. With respect to the autoantigens, our next step was to investigate the BMZ proteins, especially COL17, in

the skin and the oral mucosa.

We have shown that the greater amounts of COL17 in the oral mucosa than in the skin are associated with hemidesmosomal adhesion at the BMZ and that this compensates for the COL17 depletion induced by pemphigoid IgG. The differences in the expression level of BMZ proteins, such as COL17 may influence the clinical differences in pemphigoid.

The immunofluorescent staining demonstrated that COL17 staining was brighter in NHOM than that in NHS. This was confirmed by qPCR and immunoblotting using NHEKs and NHOMKs. The genetic shortage of COL17 is relevant to the pathogenesis of junctional epidermolysis bullosa, which shows blistering along the lamina lucida [22,56]. This indicates that the amount of hemidesmosomal COL17 is associated with the adhesion strength of basal cells anchoring to ECM. Therefore, we studied the distribution of COL17 on the plasma membrane, such as hemidesmosomes and nonhemidesmosomes. COL17 stained not only on the bottom side but also on the

lateral-apical sides of basal keratinocytes in the skin and the oral mucosa. Immunoblotting using Triton X-100-insoluble and -soluble fractions confirmed that greater amounts of COL17 were present in both the hemidesmosomes and nonhemidesmosomes of the NHOMKs than in those of the NHEKs. Given these results, we expected that the cell adhesion strength may differ between the skin and the oral mucosa. Indeed, NHOMKs showed stronger adhesion to culture plates than did NHEKs. COL17 depletion induced by BP patient IgG attenuates the cell adhesion strength [51]. In addition, COL17 knockdown induced a reduction in the number of cells adhering on the culture plate after vibration stress both in NHEKs and NHOMKs. Our results suggest that the amount of COL17 is associated with the basal cell attachment strength. We assume that the difficulty of inducing artificial separation in the oral mucosa may be attribute to the strong adhesion of the basal cells to the ECM.

The differences of BMZ proteins are expected to influence the clinical phenotype of BP. Although mAb targeting the NC16A domain depletes COL17 in both NHEKs [44] and NHOMKs (Figure 5), the clinical blisters in BP are mainly observed in the skin. The

predominant skin blistering may be related to the amount of COL17 remaining after mAb binds to COL17; i.e., the high expression of COL17 in the oral mucosa compensates for its BP-IgG-induced depletion. Pemphigus, another autoimmune blistering disease, is caused by autoantibodies against desmogleins (Dsgs). The autoantibodies targeting Dsg1 generate blisters only in the skin and not in the oral mucosa because Dsg3 is expressed throughout the oral mucosa. Conversely, autoantibodies targeting Dsg3 induce oral mucosal lesions but not skin lesions because Dsg1 counters the reduction of Dsg3 in the skin. This theory would mean that Dsg1 and Dsg3 compensate for each other in pemphigus pathogenesis [57]. Even if BP does not have exactly the same mechanism as pemphigus, the expression level of COL17 may determine the site of blister formation in BP. The blister mechanisms in BP are not simple stories, but are associated with various factors such as complement activation and inflammatory cell infiltrates [58,59]. We showed that the COL17 depletion and cell adhesion were correlated with mAb concentrations *in vitro* (Figure 11). The level of COL17 expression may not be solely associated with the blister formation in the oral mucosa, but the high autoantibody titer may involve the loss of attachment strength of

basal cell to ECM not only in the skin but also in the oral mucosa. Furthermore, the higher expression of laminin 332 may be also related to the strong adhesion in the oral mucosa due to the interaction with COL17 and laminin 332 [17]. In addition to laminin 332, various molecules such as integrin α6β4 or BP230 interact with COL17. The integrin α6/β4 were not depleted when the cells were treated by anti-COL17 antibodies [51,60], and then they may not contribute to compensation of cell detachment induced by pemphigoid IgG. In addition, BP230 should not be associated with the cell adhesion in line with the depletion of COL17 because of intracellular molecule.

Additionally, we found that IgG against the C-terminus of COL17 may have pathogenicity. IgG against regions outside the NC16A domain that are considered nonpathogenic do not induce COL17-depletion [44,52]. However, for the combination of IgG against the NC16A domain and the C-terminus, COL17-depletion was significantly enhanced (Figure 5). The enhancement of the pathogenicity by nonpathogenic IgG has been reported in pemphigus vulgaris [61] and pemphigus foliaceus [62]. The depletion activity of pathogenic mAbs against Dsg3 is known to be boosted when those mAbs act

in combination with nonpathogenic mAbs [43]. These observations are similar to our results for mAbs to the C-terminus. BP patients with IgG targeting not only the NC16A domain but also the C-terminus may show blisters on the skin and the mucosa because of the enhanced effect of anti-C-terminus IgG on COL17 depletion. A previous study has also suggested the association with autoantibodies to the C-terminus and mucosal lesions in BP [63]. Our results support the possible pathogenicity of autoantibodies targeting C-terminus.

Further step in this study is to elucidate the pathogenicity of the MMP autoantigodies targeting the C-terminous of COL17. The precise blistering mechanisms induced by autoantibodies have been well studied and include the direct inhibition of protein-protein binding by autoantibodies in pemphigus (steric hindrance) [64,65] or Fc-mediated complement and inflammatory cell activation in pemphigoid [66,67]. Steric hindrance induces the detachment of the protein-protein interactions by autoantibodies without inflammation. Therefore, we hypothesized that one of the pathogenic mechanisms for oral lesions in pemphigoid might be related to the inhibition of the

protein-protein interactions by autoantibodies with less inflammation. We focused on the interaction of COL17 with ECM proteins, especially with COL4. We found direct binding between COL4 and COL17 in normal epidermal and oral keratinocytes. In particular, this binding is disrupted by IgG against the C-terminus in oral keratinocytes. These pieces of evidence provide the novel site-specific blistering mechanisms in pemphigoid diseases.

First of all, we expected that the oral lesions in MMP would tend to be less inflammatory than the skin lesions in BP. Therefore, we compared the numbers of inflammatory infiltrating cells both in perilesions of MMP and BP. Indeed, the inflammatory cells in MMP were significantly fewer than those in BP. This observation suggests that the blistering mechanism in MMP might be dissimilar to that in BP. Hence, we focused on the interaction of COL17 with COL4. The electron microscopy and ECM binding assay [17,68] suggested that COL17 interacted with COL4 in the skin. However, the direct binding of these proteins has not been shown. Immunoprecipitaion using mAb recognizing the NC16A domain or the C-terminus clearly showed that direct

COL17-COL4 interactions exist both in NHEKs and NHOMKs. More importantly, only in NHOMKs but not in NHEKs, COL4 was not co-precipitated by mAb C17-C1. These interesting results suggest that the binding region of COL17 to COL4 may differ between in NHEKs and in NHOMKs. Furthermore, the binding may be hindered by mAb C17-C1 in NHOMKs. However, other BMZ components, such as laminin 332 or integrin α6/β4, may be interposed between COL4 and COL17 and may cause the inhibition by mAb C17-C1 in NHOMKs. This possibility was denied to show that laminin 332 and integrin α6/β4 were precipitated by both mAbs TS39-3 and C17-C1. Next, we tried to identify the precise region of COL17 interacting with COL4 using recombinant full-length COL17 and C-terminal deleted proteins. In our result, the amount of COL4 precipitated together with COL17 was relatively smaller with COL17Δ2 than with COL17Δ1. Considering the results, we suspected that the main binding site of COL17 with COL4 may be between Gly^{1175} and Asp^{1340}, in which the epitope of mAb C17-C1 (Gly^{1316}-Asp^{1340}) is located. Furthermore, COL17 may bind to COL4 in more than one domain due to the leap structure of extracellular domain of COL17 [49]. Unlike the results using NHOMKs, mAb C17-C1 co-precipitated COL4 with

COL17 in NHEK lysates. We could not elucidate the precise regions for COL17-COL4 binding in the skin.

Regarding the blistering mechanisms in oral lesions, we speculated that autoantibodies in MMP, which often target the C-terminus of COL17 [32], may inhibit the protein-protein interaction in the oral mucosa and reduce hemidesmosomal adhesions. The COL17-COL4 binding was inhibited by mAb C17-C1 targeting the C-terminus of COL17. This is a similar finding to pemphigus. It is reported that a pathogenic mAb against Dsg 3 (mAb AK23) causes direct inhibition of Dsg 3 interactions (steric hindrance) [69]. In the present study, we showed that MMP-IgG hinders the binding of COL17 with COL4, similar to mAb C17-C1. Furthermore, MMP autoantibodies share the epitope of mAb C17-C1 by competitive COL17-ELISA. Finally, we demonstrated that the cell adhesion strength was reduced by the treatment of mAb C17-C1 in NHOMKs. Based on our results, we hypothesize the blistering mechanisms; autoantibodies against C-terminus of COL17 hinder the binding of COL17 and COL4 in oral mucosa.

The autoantigens of MMP are reported to be not merely COL17 but also laminin 332, integrin α6β4, and collagen VII [24]. Recently, an MMP mouse model was reported in which the disease was induced by injection with anti-mouse laminin α3 IgG [70]. Mice injected with IgG developed erosions and crusts not just on the skin but also on the conjunctival, oral and pharyngeal mucosa. The clinical manifestation of this MMP mouse model was Fc receptor-dependent and complement-dependent, similar to previous BP mouse models [58,59,71]. In contrast, non-inflammatory mechanisms of BP were also proposed [72]. BP patient IgG against NC16A significantly induces COL17 depletion in cultured keratinocytes and BP patient skin. COL17 depletion is important for the blistering along the lamina densa without inflammation. Compared to NC16A-IgG, IgG targeting the C-terminus, including MMP-IgG, does not induce COL17 depletion. Our results suggest that the blistering mechanisms in COL17-type MMP are distinctive from those in BP. A recent study revealed that BP patients with normal eosinophil counts presented mucous lesions more frequently than those with higher eosinophila [73]. Furthermore, oral mucosal lesions in some pemphigoid patients

were associated with the administration of DPP-4i [43, 44]. A certain HLA allele (HLA-DQB1*03:01) was associated with a high risk of DDP-4i BP and MMP occurrence [74,25]. In light of this evidence, oral mucosal lesions in pemphigoid may be related to be less inflammatory associated with a certain HLA allele .

To summarize, we correlate the differences of COL17 between the skin and the oral mucosa with the site of blister formation in pemphigoid. We show that the greater amounts of COL17 in the oral mucosa than in the skin are associated with hemidesmosomal adhesion at the BMZ and that this compensates for the COL17 depletion induced by pemphigoid IgG. The differences in the expression level of BMZ proteins, such as COL17 and laminin 332, may influence the clinical differences in pemphigoid.

Furthermore, we provide a novel finding that COL17 directly binds to COL4 at the BMZ in the keratinocytes. mAb targeting the C-terminus of COL17 or MMP-IgG disrupts the binding of COL17 and COL4 in NHOMKs. Pemphigoid IgG targeting the C-terminus of COL17 may play a pathogenic role in the blistering formation in the oral

mucosa to inhibit protein-protein interactions with less inflammation. However, the pathogenesis of the autoantibodies against the C-terminus of COL17 has needed further investigations. It is our hope that the findings in this study may shed light on the unanswered questions in this field, and lead to further understandings and innovative therapy for these diseases.

References

1 Stephens P, Genever P. Non-epithelial oral mucosal progenitor cell populations. *Oral Dis* 2007; **13**:1–10.

2 Shetty S, Gokul S. Keratinization and its disorders. *Oman Med J* 2012; **27**:348–57.

3 Brandtzaeg P. Secretory IgA: Designed for Anti-Microbial Defense. *Front Immunol* 2013; **4**:222.

4 Turabelidze A, Guo S, Chung AY, *et al.* Intrinsic differences between oral and skin keratinocytes. *PLoS ONE* 2014; **9**:e101480.

5 Drukała J, Zarzecka J, Gojniczek K, *et al.* Comparison of proliferation and motile activity between human keratinocytes isolated from skin and oral mucosa. *Folia Biol (Krakow)* 2005; **53**:21–8.

6 Kim HS, Kim NH, Kim J, Cha IH. Inducing re-epithelialization in skin wound through cultured oral mucosal keratinocytes. *J Korean Assoc Oral Maxillofac Surg* 2013; **39**:63–70.

7 Borradori L, Sonnenberg A. Structure and function of hemidesmosomes: more than simple adhesion complexes. *J Invest Dermatol* 1999; **112**:411–8.

8 Green KJ, Jones JC. Desmosomes and hemidesmosomes: structure and function of molecular components. *FASEB J* 1996; **10**:871–81.

9 Jones JC, Hopkinson SB, Goldfinger LE. Structure and assembly of hemidesmosomes. *Bioessays* 1998; **20**:488–94.

10 Walko G, Castañón MJ, Wiche G. Molecular architecture and function of the hemidesmosome. *Cell Tissue Res* 2015; **360**:363–78.

11 Sugawara K, Tsuruta D, Ishii M, *et al.* Laminin-332 and -511 in skin. *Exp Dermatol* 2008; **17**:473–80.

12 Aumailley M, Smyth N. The role of laminins in basement membrane function. *J Anat* 1998; **193 (Pt 1)**:1–21.

13 Keene DR, Sakai LY, Lunstrum GP, *et al.* Type VII collagen forms an extended network of anchoring fibrils. *J Cell Biol* 1987; **104**:611–21.

14 Woodley DT, Briggaman RA, O'Keefe EJ, *et al.* Identification of the skin basement-membrane autoantigen in epidermolysis bullosa acquisita. *N Engl J Med* 1984; **310**:1007–13.

15 Hopkinson SB, Findlay K, deHart GW, Jones JC. Interaction of BP180 (type XVII collagen) and alpha6 integrin is necessary for stabilization of hemidesmosome structure. *J Invest Dermatol* 1998; **111**:1015–22.

16 Tasanen K, Tunggal L, Chometon G, *et al.* Keratinocytes from patients lacking collagen XVII display a migratory phenotype. *Am J Pathol* 2004; **164**:2027–38.

17 Nishie W, Kiritsi D, Nyström A, *et al.* Dynamic interactions of epidermal collagen XVII with the extracellular matrix: laminin 332 as a major binding partner. *Am J Pathol* 2011; **179**:829–37.

18 Koster J, Geerts D, Favre B, *et al.* Analysis of the interactions between BP180, BP230, plectin and the integrin alpha6beta4 important for hemidesmosome assembly. *J Cell Sci* 2003; **116**:387–99.

19 Hopkinson SB, Jones JC. The N terminus of the transmembrane protein BP180 interacts with the N-terminal domain of BP230, thereby mediating keratin cytoskeleton anchorage to the cell surface at the site of the hemidesmosome. *Mol Biol Cell* 2000; **11**:277–86.

20 Natsuga K, Nishie W, Nishimura M, *et al.* Loss of interaction between plectin and type XVII collagen results in epidermolysis bullosa simplex. *Hum Mutat* 2017; **38**:1666–70.

21 Aho S, Uitto J. Direct interaction between the intracellular domains of bullous pemphigoid antigen 2 (BP180) and beta 4 integrin, hemidesmosomal components of basal keratinocytes. *Biochem Biophys Res Commun* 1998; **243**:694–9.

22 Fine J-D, Bruckner-Tuderman L, Eady RAJ, *et al.* Inherited epidermolysis bullosa: updated recommendations on diagnosis and classification. *J Am Acad Dermatol* 2014; **70**:1103–26.

23 Schmidt E, Zillikens D. Pemphigoid diseases. *The Lancet* 2013; **381**:320–32.

24 Amber KT, Murrell DF, Schmidt E, *et al.* Autoimmune Subepidermal Bullous Diseases of the Skin and Mucosae: Clinical Features, Diagnosis, and Management. *Clin Rev Allergy Immunol* 2017; **381**:320–6.

25 Bernard P, Antonicelli F. Bullous Pemphigoid: A Review of its Diagnosis, Associations and Treatment. *Am J Clin Dermatol* 2017; **18**:513–28.

26 Murrell DF, Marinovic B, Caux F, *et al.* Definitions and outcome measures for mucous membrane pemphigoid: recommendations of an international panel of experts., 2015; 168–74.

27 Vorobyev A, Ludwig RJ, Schmidt E. Clinical features and diagnosis of epidermolysis bullosa acquisita. *Expert Rev Clin Immunol* 2017; **13**:157–69.

28 Xu H-H, Werth VP, Parisi E, Sollecito TP. Mucous membrane pemphigoid. *Dent Clin North Am* 2013; **57**:611–30.

29 Rashid KA, Foster CS, Ahmed AR. Identification of epitopes within integrin β4 for binding of auto-antibodies in ocular cicatricial and mucous membrane pemphigoid: preliminary report. *Invest Ophthalmol Vis Sci* 2013; **54**:7707–16.

30 Giudice GJ, Emery DJ, Diaz LA. Cloning and primary structural analysis of the bullous pemphigoid autoantigen BP180. *J Invest Dermatol* 1992; **99**:243–50.

31 Di Zenzo G, Grosso F, Terracina M, *et al.* Characterization of the anti-BP180 autoantibody reactivity profile and epitope mapping in bullous pemphigoid patients. *J Invest Dermatol* 2004; **122**:103–10.

32 Schmidt E, Skrobek C, Kromminga A, *et al.* Cicatricial pemphigoid: IgA and IgG autoantibodies target epitopes on both intra- and extracellular domains of bullous pemphigoid antigen 180. *Br J Dermatol* 2001; **145**:778–83.

33 Kamaguchi M, Iwata H, Ujiie H, *et al.* Oral mucosa is a useful substrate for detecting autoantibodies of mucous membrane pemphigoid. *Br J Dermatol* 2017. doi:10.1111/bjd.15925.

34 Kamaguchi M, Iwata H, Ujiie H, *et al.* High Expression of Collagen XVII Compensates for Its Depletion Induced by Pemphigoid IgG in the Oral Mucosa. *J Invest Dermatol* 2018. doi:10.1016/j.jid.2018.03.002.

35 Izumi K, Nishie W, Mai Y, *et al.* Autoantibody Profile Differentiates between Inflammatory and Noninflammatory Bullous Pemphigoid. *J Invest Dermatol* 2016; **136**:2201–10.

36 Kamaguchi M, Iwata H, Ujiie I, *et al.* Direct Immunofluorescence Using Non-Lesional Buccal Mucosa in Mucous Membrane Pemphigoid. *Front Med (Lausanne)* 2018; **5**:20.

37 Gammon WR, Fine JD, Forbes M, Briggaman RA. Immunofluorescence on split skin for the detection and differentiation of basement membrane zone autoantibodies. *J Am Acad Dermatol* 1992; **27**:79–87.

38 Nishie W, Sawamura D, Goto M, *et al.* Humanization of autoantigen. *Nat Med* 2007; **13**:378–83.

39 Toyonaga E, Nishie W, Izumi K, *et al.* C-terminal processing of collagen XVII induces neoepitopes for linear IgA dermatosis autoantibodies. *J Invest Dermatol* 2017. doi:10.1016/j.jid.2017.07.831.

40 Hybbinette S, Boström M, Lindberg K. Enzymatic dissociation of keratinocytes from human skin biopsies for in vitro cell propagation. *Exp Dermatol* 1999; **8**:30–8.

41 Ujiie H, Sasaoka T, Izumi K, *et al.* Bullous pemphigoid autoantibodies directly induce blister formation without complement activation. *J Immunol* 2014; **193**:4415–28.

42 Hirako Y, Yonemoto Y, Yamauchi T, *et al.* Isolation of a hemidesmosome-rich fraction from a human squamous cell carcinoma cell line. *Experimental Cell Research* 2014; **324**:172–82.

43 Yamamoto Y, Aoyama Y, Shu E, *et al.* Anti-desmoglein 3 (Dsg3) monoclonal antibodies deplete desmosomes of Dsg3 and differ in their Dsg3-depleting activities related to pathogenicity. *J Biol Chem* 2007; **282**:17866–76.

44 Wada M, Nishie W, Ujiie H, *et al.* Epitope-Dependent Pathogenicity of Antibodies Targeting a Major Bullous Pemphigoid Autoantigen Collagen XVII/BP180. *J Invest Dermatol* 2016; **136**:938–46.

45 Glim JE, Everts V, Niessen FB, *et al.* Extracellular matrix components of oral mucosa differ from skin and resemble that of foetal skin. *Arch Oral Biol* 2014; **59**:1048–55.

46 Kitajima Y, Owaribe K, Nishizawa Y, *et al.* Phorbol ester- and calcium-induced reorganization of 180-kDa bullous pemphigoid antigen on the ventral surface of cultured human keratinocytes as studied by immunofluorescence and immunoelectron microscopy. *Experimental Cell Research* 1992; **203**:17–24.

47 Hirako Y, Usukura J, Uematsu J, *et al.* Cleavage of BP180, a 180-kDa bullous pemphigoid antigen, yields a 120-kDa collagenous extracellular polypeptide. *J Biol Chem* 1998; **273**:9711–7.

48 Watanabe M, Natsuga K, Nishie W, *et al.* Type XVII collagen coordinates proliferation in the interfollicular epidermis. *Elife* 2017; **6**:a015206.

49 Masunaga T, Shimizu H, Yee C, *et al.* The extracellular domain of BPAG2 localizes to anchoring filaments and its carboxyl terminus extends to the lamina densa of normal human epidermal basement membrane. *J Invest Dermatol* 1997; **109**:200–6.

50 McMillan JR, Akiyama M, Nakamura H, Shimizu H. Colocalization of multiple laminin isoforms predominantly beneath hemidesmosomes in the upper lamina densa of the epidermal basement membrane. *J Histochem Cytochem* 2006; **54**:109–18.

51 Iwata H, Kitajima Y, Kamio N, *et al.* IgG from Patients with Bullous Pemphigoid Depletes Cultured Keratinocytes of the 180-kDa Bullous Pemphigoid Antigen (Type XVII Collagen) and Weakens Cell Attachment. *J Invest Dermatol* 2009; **129**:919–26.

52 Imafuku K, Iwata H, Kamaguchi M, *et al.* Autoantibodies of non-inflammatory bullous pemphigoid hardly deplete type XVII collagen of keratinocytes. *Exp Dermatol* 2017; **381**:320.

53 Natsuga K, Natsuga K, Nishie W, *et al.* Antibodies to pathogenic epitopes on type XVII collagen cause skin fragility in a complement-dependent and -independent manner. *J Immunol* 2012; **188**:5792–9.

54 Li Q, Ujiie H, Shibaki A, *et al.* Human IgG1 monoclonal antibody against human collagen 17 noncollagenous 16A domain induces blisters via complement activation in experimental bullous pemphigoid model. *J Immunol* 2010; **185**:7746–55.

55 Iwata H, Kitajima Y. Bullous pemphigoid: role of complement and mechanisms for blister formation within the lamina lucida. *Exp Dermatol* 2013; **22**:381–5.

56 McGrath JA, Gatalica B, Christiano AM, *et al.* Mutations in the 180-kD bullous pemphigoid antigen (BPAG2), a hemidesmosomal transmembrane collagen (COL17A1), in generalized atrophic benign epidermolysis bullosa. *Nat Genet* 1995; **11**:83–6.

57 Mahoney MG, Wang Z, Rothenberger K, *et al.* Explanations for the clinical and microscopic localization of lesions in pemphigus foliaceus and vulgaris. *J Clin Invest* 1999; **103**:461–8.

58 Liu Z, Giudice GJ, Swartz SJ, *et al.* The role of complement in experimental bullous pemphigoid. *J Clin Invest* 1995; **95**:1539–44.

59 Liu Z, Giudice GJ, Zhou X, *et al.* A major role for neutrophils in experimental bullous pemphigoid. *J Clin Invest* 1997; **100**:1256–63.

60 Kamaguchi M, Iwata H, Mori Y, *et al.* Anti-idiotypic Antibodies against BP-IgG Prevent Type XVII Collagen Depletion. *Front Immunol* 2017; **8**:1669.

61 Kawasaki H, Tsunoda K, Hata T, *et al.* Synergistic pathogenic effects of combined mouse monoclonal anti-desmoglein 3 IgG antibodies on pemphigus vulgaris blister formation. *J Invest Dermatol* 2006; **126**:2621–30.

62 Yoshida K, Ishii K, Shimizu A, *et al.* Non-pathogenic pemphigus foliaceus (PF) IgG acts synergistically with a directly pathogenic PF IgG to increase blistering by p38MAPK-dependent desmoglein 1 clustering. *J Dermatol Sci* 2017; **85**:197–207.

63 Hofmann S, Thoma-Uszynski S, Hunziker T, *et al.* Severity and phenotype of bullous pemphigoid relate to autoantibody profile against the NH2- and COOH-terminal regions of the BP180 ectodomain. *J Invest Dermatol* 2002; **119**:1065–73.

64 Tsunoda K, Ota T, Aoki M, *et al.* Induction of pemphigus phenotype by a mouse monoclonal antibody against the amino-terminal adhesive interface of desmoglein 3. *J Immunol* 2003; **170**:2170–8.

65 Ishii K, Harada R, Matsuo I, *et al.* In vitro keratinocyte dissociation assay for evaluation of the pathogenicity of anti-desmoglein 3 IgG autoantibodies in pemphigus vulgaris. *J Invest Dermatol* 2005; **124**:939–46.

66 Iwata H, Bieber K, Hirose M, Ludwig RJ. Animal models to investigate pathomechanisms and evaluate novel treatments for autoimmune bullous dermatoses. *Curr Pharm Des* 2015; **21**:2422–39.

67 Ludwig RJ, Vanhoorelbeke K, Leypoldt F, *et al.* Mechanisms of Autoantibody-Induced Pathology. *Front Immunol* 2017; **8**:603.

68 Nonaka S, Ishiko A, Masunaga T, *et al.* The extracellular domain of BPAG2 has a loop structure in the carboxy terminal flexible tail in vivo. *J Invest Dermatol* 2000; **115**:889–92.

69 Saito M, Stahley SN, Caughman CY, *et al.* Signaling dependent and independent mechanisms in pemphigus vulgaris blister formation. *PLoS ONE* 2012; **7**:e50696.

70 Heppe EN, Tofern S, Schulze FS, *et al.* Experimental laminin 332 mucous membrane pemphigoid critically involves C5aR1 and reflects clinical and immunopathological characteristics of the human disease. *J Invest Dermatol* 2017. doi:10.1016/j.jid.2017.03.037.

71 Schulze FS, Beckmann T, Nimmerjahn F, *et al.* Fcγ receptors III and IV mediate tissue destruction in a novel adult mouse model of bullous pemphigoid. *Am J Pathol* 2014; **184**:2185–96.

72 Iwata H, Ujiie H. Complement-independent blistering mechanisms in bullous pemphigoid. *Exp Dermatol* 2017. doi:10.1111/exd.13367.

73 Kridin K. Peripheral eosinophilia in bullous pemphigoid: Prevalence and influence on the clinical manifestation. *Br J Dermatol* 2018. doi:10.1111/bjd.16679.

74 Ujiie H, Muramatsu K, Mushiroda T, *et al.* HLA-DQB1*03:01 as a Biomarker for Genetic Susceptibility to Bullous Pemphigoid Induced by DPP-4 Inhibitors. *J Invest Dermatol* 2017. doi:10.1016/j.jid.2017.11.023.

Figure legends

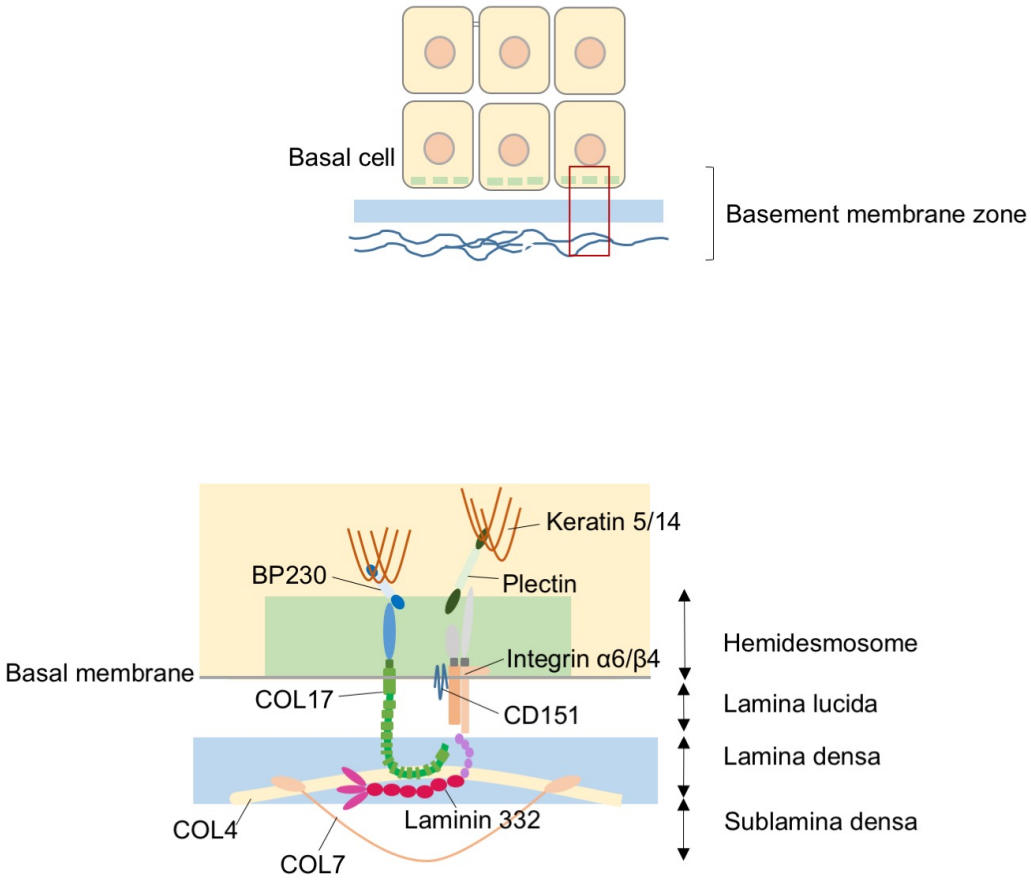

Figure 1 Structure of basement membrane zone

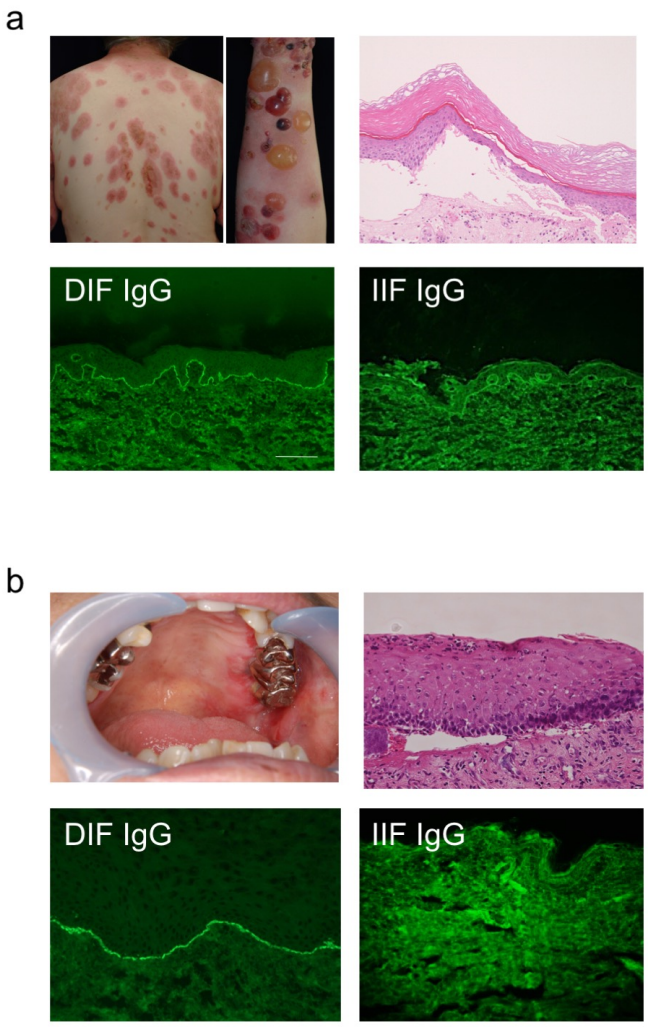

Figure 2 Representative clinical and immunofluorescent findings of MMP and BP.

a) BP patients. Multiple blisters associated with erythema are seen (upper-left). Histological analyses shows junctional separation at the basement membrane zone (upper-right). DIF reveals linear IgG deposition along the BMZ (lower-left). IIF using normal human skin detected circulating IgG to BMZ (lower-right). b) MMP patient. The erosion is observed in tha maxillry gingiva (upper-left). Histological analyses shows junctional separation at the basement membrane zone (upper-right).DIF reveals linear deposition of IgG along the BMZ (lower-left). IIF using normal human skin does not detect the circulating IgG to BMZ (lower-right). H&E: hematoxylin and eosin staining. scale bars; 100 μ m

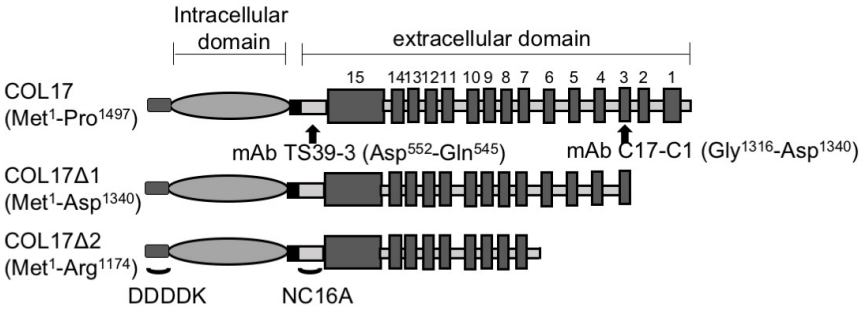

Figure 3 Schema of full-length human COL17 and recombinant C-terminal-deleted COL17 (COL17Δ1, COL17Δ2) expressed by HEK293 cells.

The epitopes of mAb TS39-3 (Asp^{552}-Gln^{545}) and mAb C17-C1 (Gly^{1316}-Asp^{1340}) are indicated.

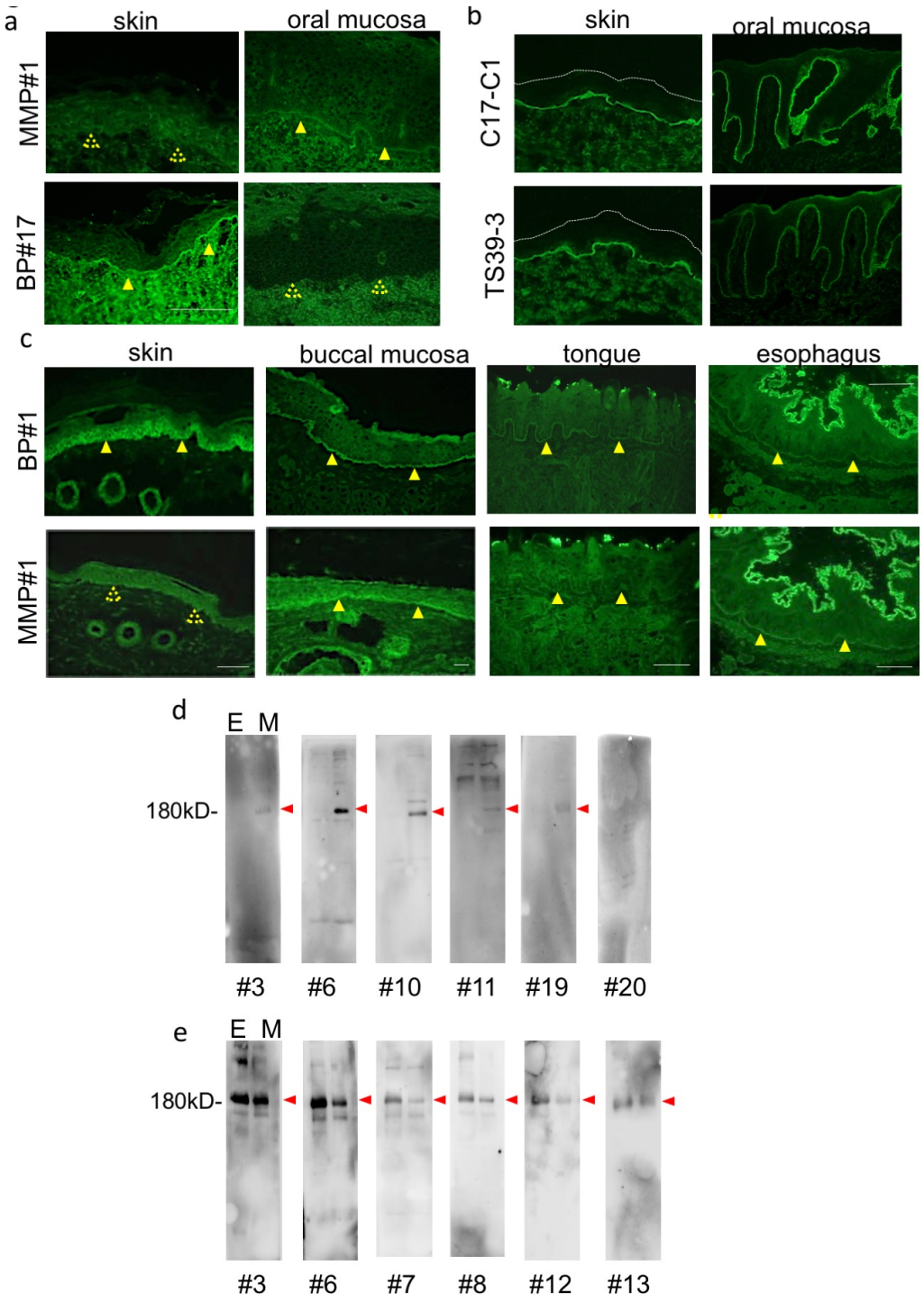

Figure 4 BP and MMP autoantibodies react differently to the skin and the oral mucosal substrates

a) Indirect immunofluorescence of normal human skin and mucosal substrates. The sera of MMP case 1 shows positive reactivity against BMZ in normal human oral mucosa (arrow heads), but not in skin (dotted arrow heads). In contrast, BP case 17 shows positive reactivity against the BMZ in normal human skin (arrow heads), but not in oral mucosa (dotted arrow heads). (b) The mAbs TS39-3 and C17-C1 target the NC16A domain and the C-terminus of human COL17 domain. The sections of normal human skin and oral mucosa were stained with mAb TS39-3 and mAb C17-C1 at 0.003 mg/ml. Subsequently, sections were incubated with FITC-conjugated anti-mouse IgG. Two substrates of skin and mucosa were used for the experiments. scale bars; 50 μm (c) IIF using COL 17 humanized mouse organ samples, (skin, buccal mucosa, tongue, esophagus). scale bars; 100 μm d) Immunoblotting using NHEKs and NHOMKs
Immunoblotting was performed using NHEK and NHOMK lysate as substrates. Membranes were incubated with 1.10 diluted sera, followed by incubation with HRP-conjugated anti-human IgG. Representative immunoblotting pictures of MMP sera (a), and BP sera (b) are shown. E; NHEK lysate, M; NHOMK lysate.

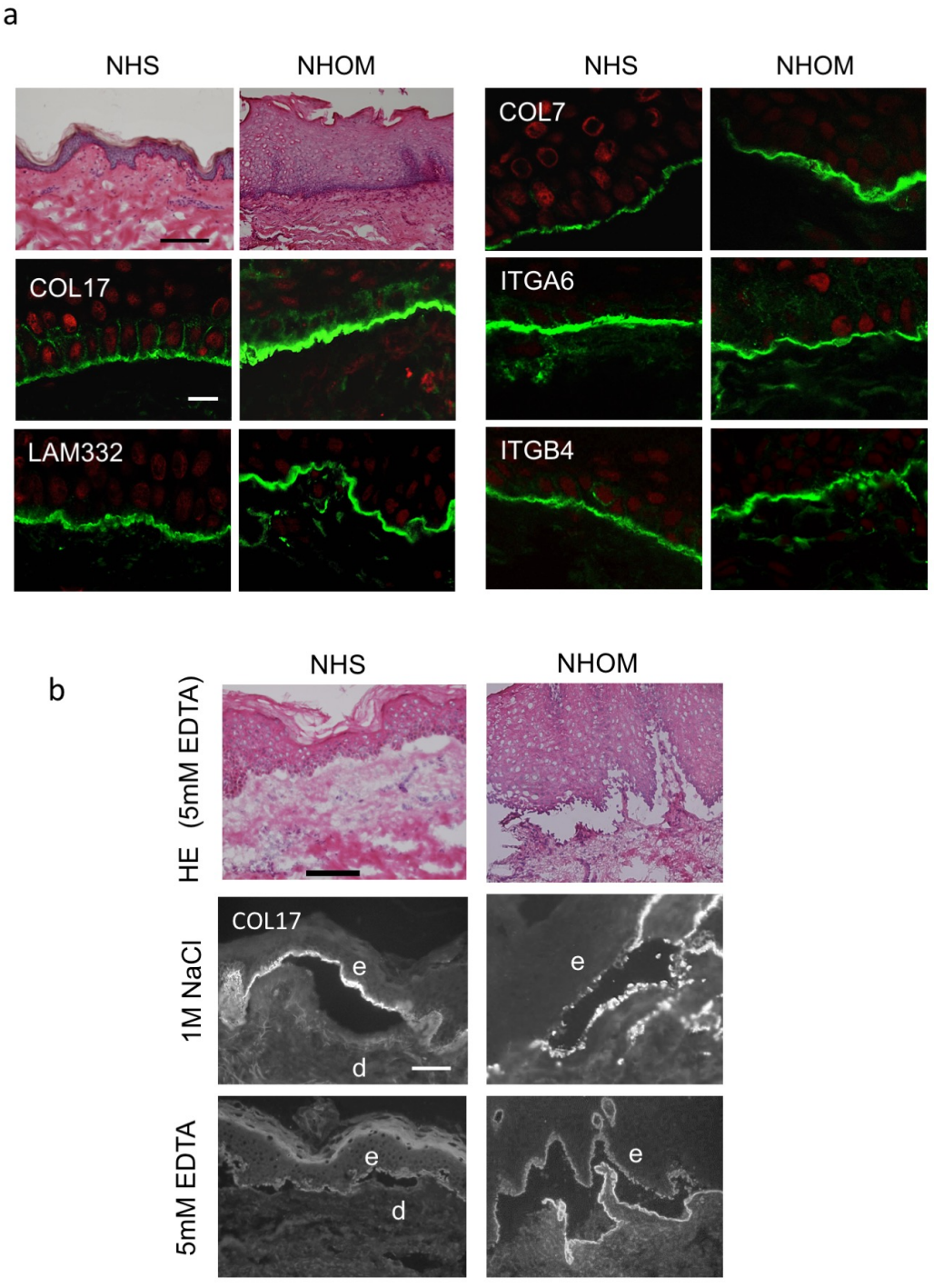

Figure 5 Immunofluorescent staining of BMZ proteins, and Artificial split formation treated with 1 M NaCl or 5 mM EDTA in the skin and oral mucosa

a) Hematoxylin and eosin (H&E) staining were performed on NHS and NHOM. For immunofluorescent staining, NHS and NHOM were stained with anti-COL17, anti-laminin 332 (LAM332), anti-COL7, anti-integrin α6 (ITGA6), or anti-integrin β4 (ITGB4), followed by staining with FITC-conjugated anti-mouse, anti-rabbit or anti-rat IgG. The nuclei were stained with propidium iodide. Images were taken by confocal laser scanning microscope (n=3). H&E staining, scale bar: 200 μm. Immunofluorescent staining, scale bar: 10 μm. b) Artificial dermal-epidermal separations on NHS (left panels) and NHOM (right panels) were created by incubation with 1 M NaCl or 5 mM EDTA. H&E staining and immunofluorescent staining of COL17 were performed on NHS and NHOM (n=3). e: epidermis (NHS), epithelium (NHOM), d: dermis (NHS), l: lamina propria (NHOM). Scale bars: 100 μm

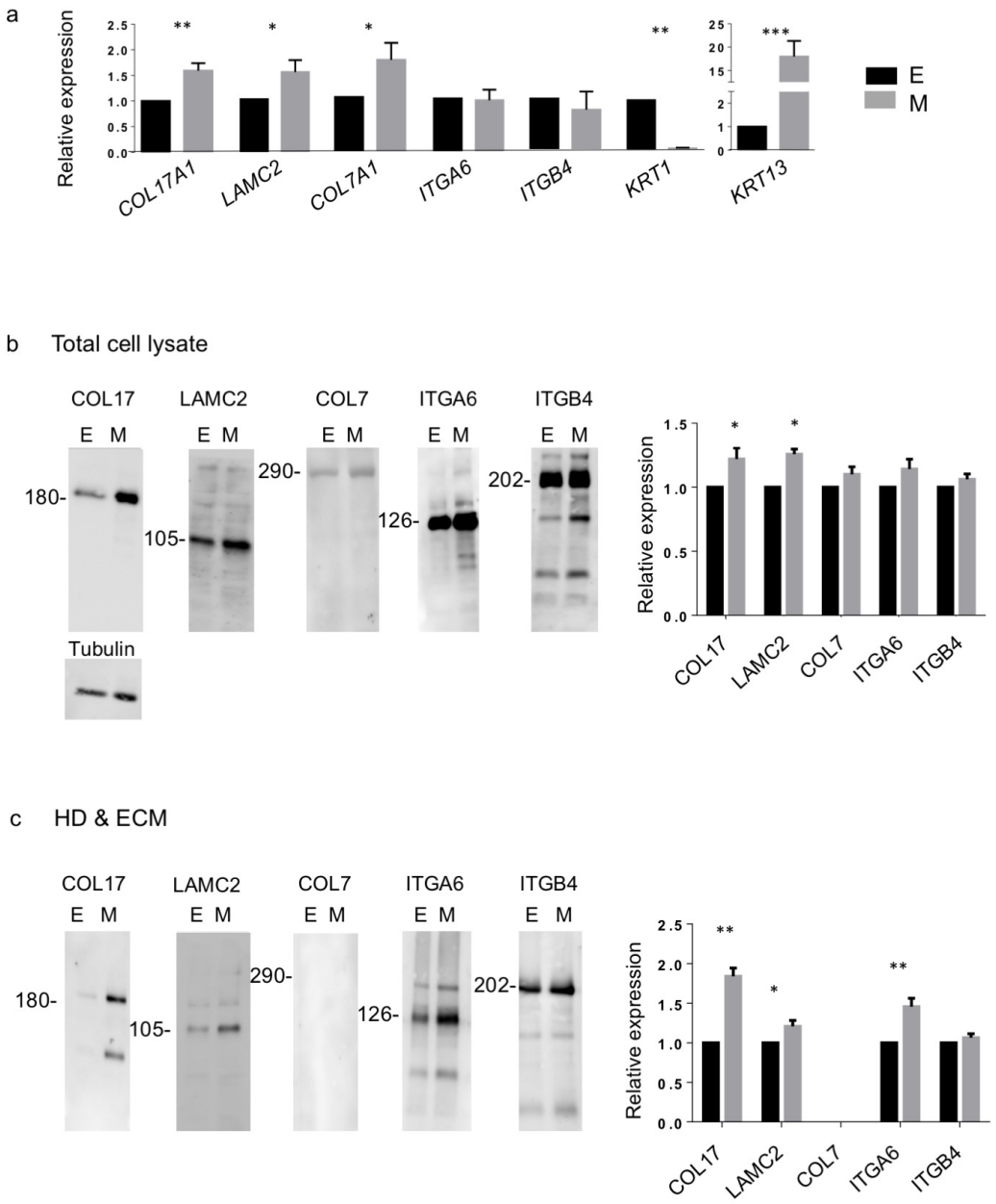

Figure 6 Figure 3 mRNA and protein expression of BMZ proteins in NHEKs and NHOMKs

(a) The gene expression levels of *COL17A1, LAMC2, COL7A1, ITGA6, ITGB4, KRT1,* and *KRT13* in NHOMKs are compared to those in NHEKs (n=3). Immunoblotting using (b) total cell lysate, (c) hemidesmosome and ECM fraction (HD & ECM) of NHEKs and NHOMKs detecting COL17, laminin γ2 (LAMC2), COL7, integrin α6 (ITGA6), or integrin β4 (ITGB4) (n=3). The data are expressed as the mean ± S.D. Student's *t*-test. *0.01<p<0.05, **0.001<p<0.01, ***0.0001<p<0.001, ****p<0.0001.

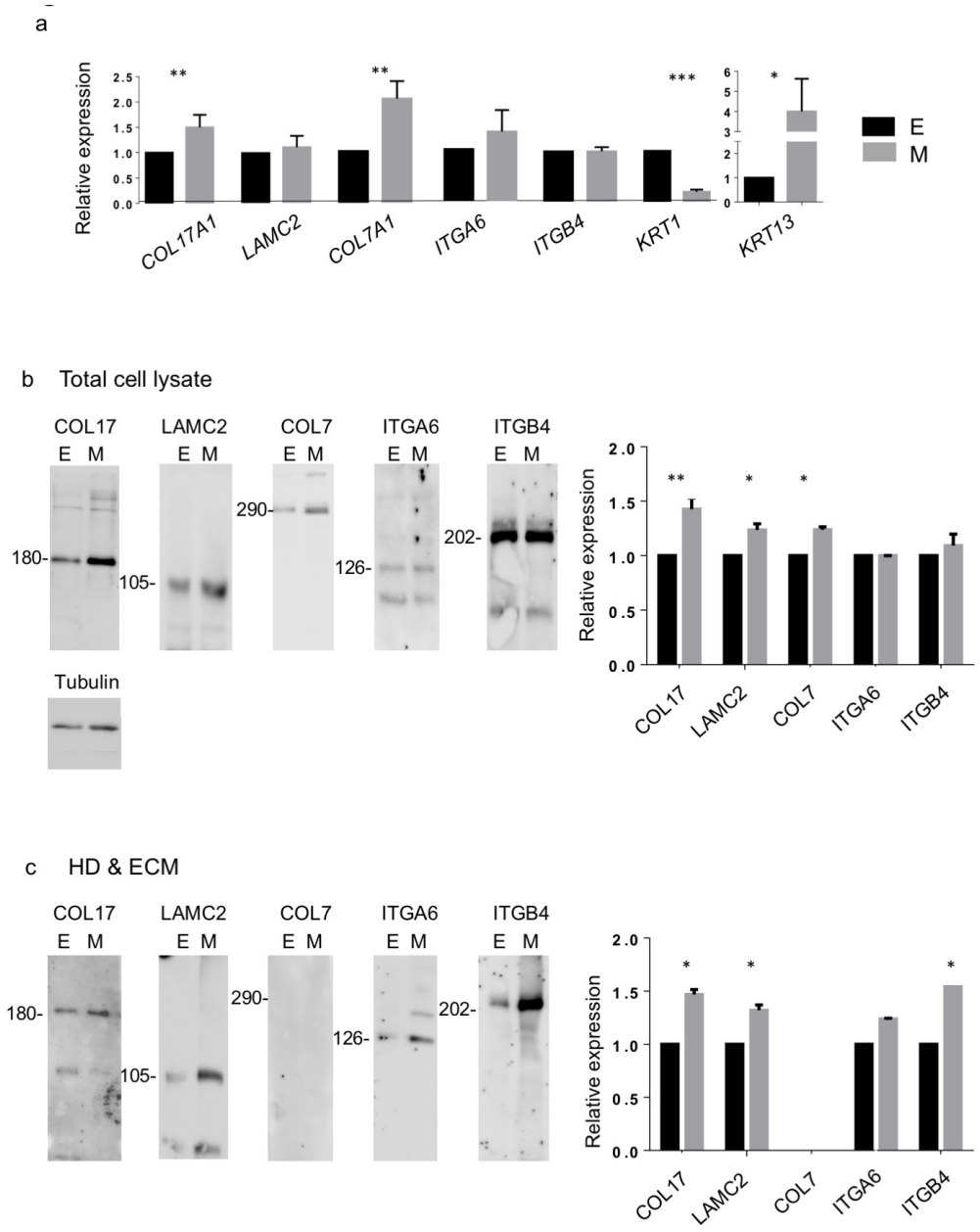

Figure 7 mRNA and protein expression of BMZ proteins in NHEK and NHOMK in a single individual

(a) The gene expression levels of *COL17A1, COL7A1, LAMC2, ITGA6, ITGB4, KRT1,* and *KRT13* in NHOMKs compared to those levels in NHEKs. Immunoblotting detecting COL17, COL7, laminin γ2 (LAMC2), integrin α6 (ITGA6) and integrin β4 (ITGB4) using (b) total cell lysates and (c) hemidesmosome & ECM fraction (HD & ECM) of NHEKs and NHOMKs. The data are expressed as the mean ±S.D. Student's *t*-test. *0.01<p<0.05, **0.001<p<0.01, ***0.0001<p<0.001, ****p<0.0001.

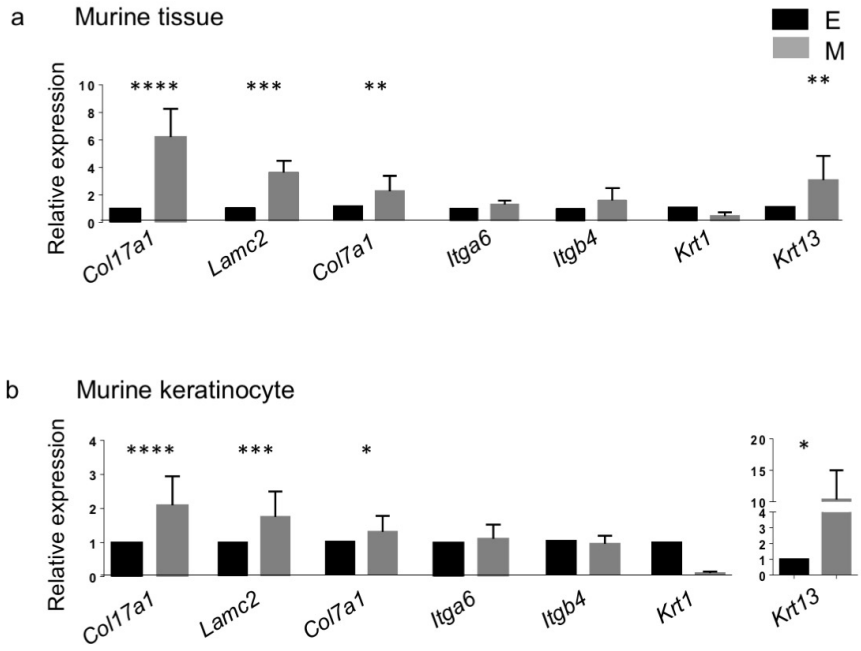

Figure 8 mRNA expression of BMZ proteins of murine tissue and keratinocytes

The gene expression levels of *Col17a1, Col7a1, Lamc2, Itga6, Itgb4, Krt1* and *Krt13* extracted from (a) murine tissue (tail skin and buccal mucosa) (n=5) and from (b) murine keratinocytes (tail skin and buccal mucosa) (n=4). The data are expressed as the mean ±S.D. Student's *t*-test. *0.01<p<0.05, **0.001<p<0.01, ***0.0001<p<0.001, ****p<0.0001.

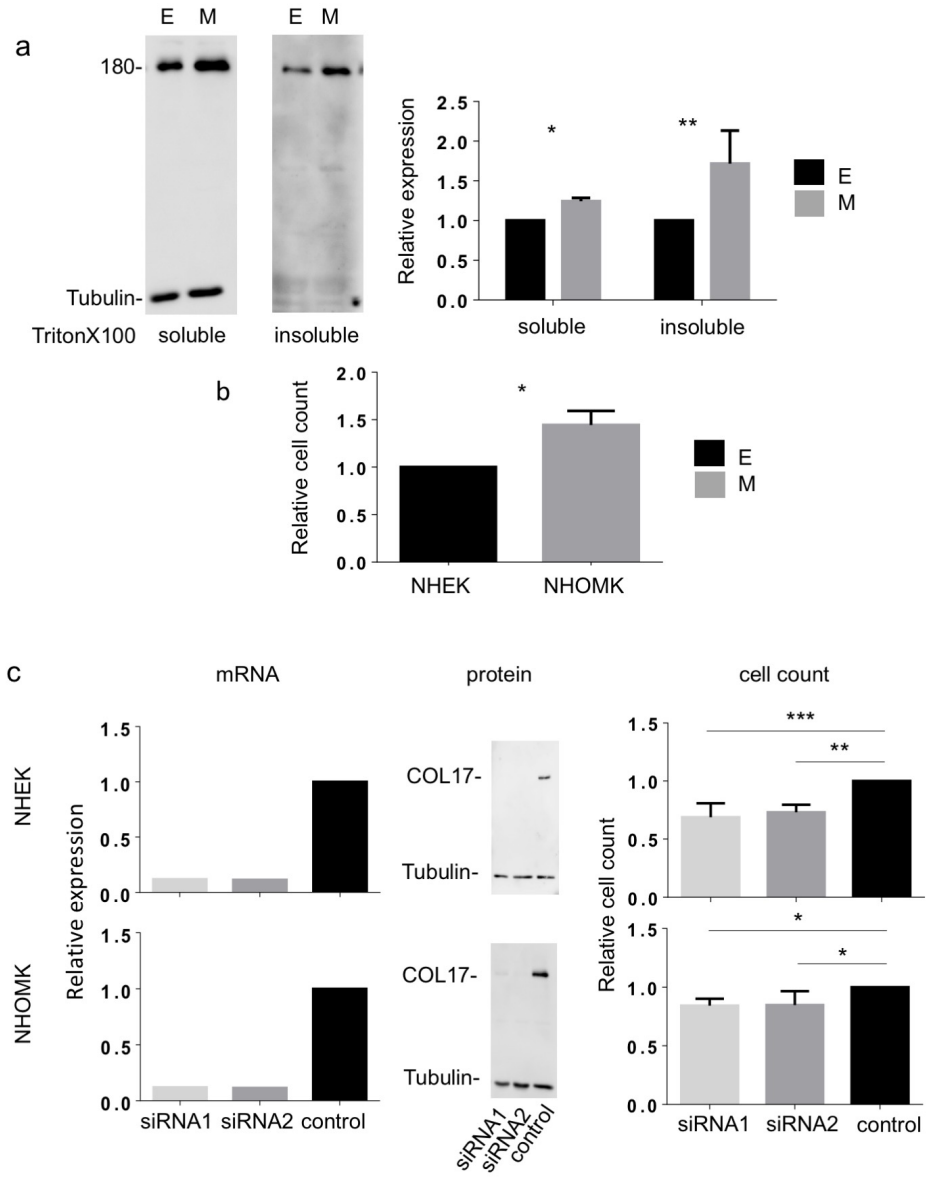

Figure 9 Immunoblotting of Triton X-100-soluble and -insoluble fractions and cell adhesion test

a) Immunoblotting of COL17 using Triton X-100-soluble and -insoluble fractions from NHEKs and NHOMKs (n=3). (b) Culture plates were placed on the vortex for 20 minutes, and the remaining cells were counted (n=2). (c) Cell adhesion strength was tested using NHEKs and NHOMKs treated with COL17 knockdown (n=3). The data are expressed as the mean ± S.D. Student's *t*-test. *0.01<p<0.05, **0.001<p<0.01, ***0.0001<p<0.001, ****p<0.0001.

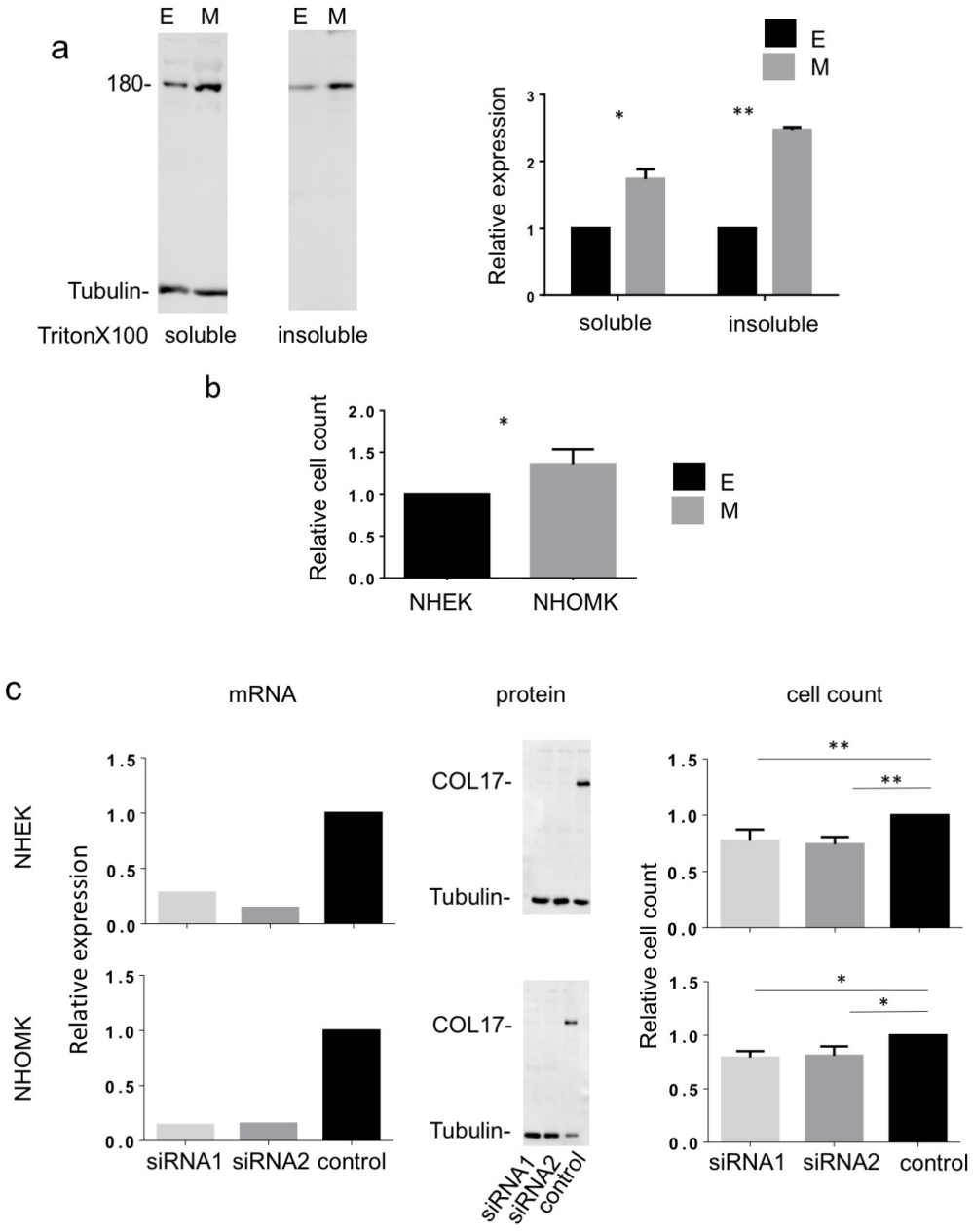

Figure 10 Immunoblotting of Triton X-100-soluble and -insoluble fractions and cell adhesion test in a single individual

(a) Immunoblotting of COL17 using Triton X-100-soluble fraction and -insoluble fraction from NHEKs and NHOMKs. (b) Cell adhesion strength was investigated using NHEKs and NHOMKs. (c) Cell adhesion strength was investigated using COL17-knockdown NHEKs and NHOMKs. The data are expressed as the mean ±S.D. Student's *t*-test. *0.01<p<0.05, **0.001<p<0.01, ***0.0001<p<0.001, ****p<0.0001.

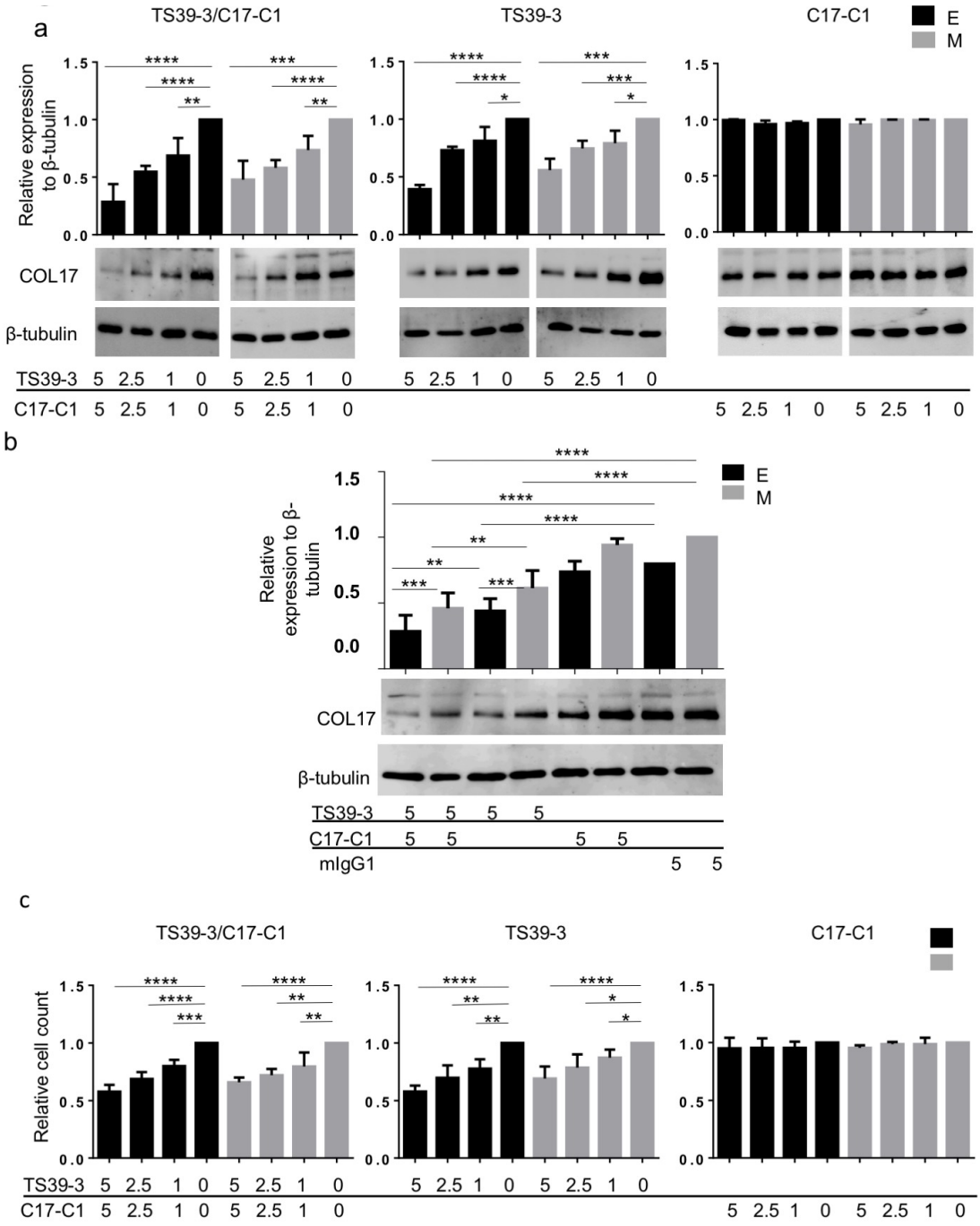

Figure 11 COL17 depletion in keratinocytes treated with mAbs against COL17

a) NHEKs and NHOMKs were treated with mAbs TS39-3, C17-C1 or a combination of mAbs TS39-3 and C17-C1 with the concentrations of 5, 2.5, 1, 0 µg/ml (n=3). The graph shows the COL17 amount relative to the β-tubulin (upper panels). The representative immunoblotting is presented (lower panels). b)NHEKs and NHOMKs were treated with mAbs TS39-3, C17-C1 or mIgG1 and a combination of mAbs TS39-3 and C17-C1. The total concentration of each treatment was 2.5 µg/ml (n=5). The graph

shows the COL17 amount relative to the β-tubulin (upper panels). The representative immunoblotting is presented (lower panels). c) Cell adhesion strength was tested using NHEKs and NHOMKs treated with mAbs TS39-3, C17-C1 or a combination of mAbs, TS39-3, and C17-C1 with the concentrations of 5, 2.5, 1, 0 μg/ml (n=3). The data are expressed as the mean ± S.D. One-way ANOVA. *$0.01<p<0.05$, **$0.001<p<0.01$, ***$0.0001<p<0.001$, ****$p<0.0001$.

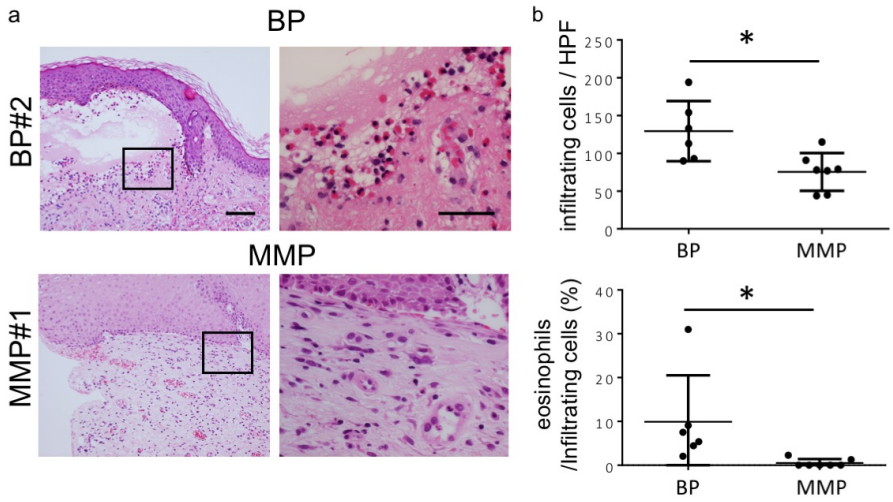

Figure 12 Oral lesions in MMP are less inflammatory than skin lesion in BP

(a) Representative histopathological findings of typical BP patients with autoantibodies against NC16A and MMP are shown. H&E staining, scale bar=100 μm (left). The black square indicates the area of 220 × 180 μm square under ×400 magnification high-power field (HPF), scale bare=50 μm (right). (b) Comparison of the total number of infiltrating cells (upper) and percentage of eosinophils (lower) between BP (n=6) and MMP (n=7). The data are expressed as the mean ± S.D. Student's *t*-test. *0.01<p<0.05.

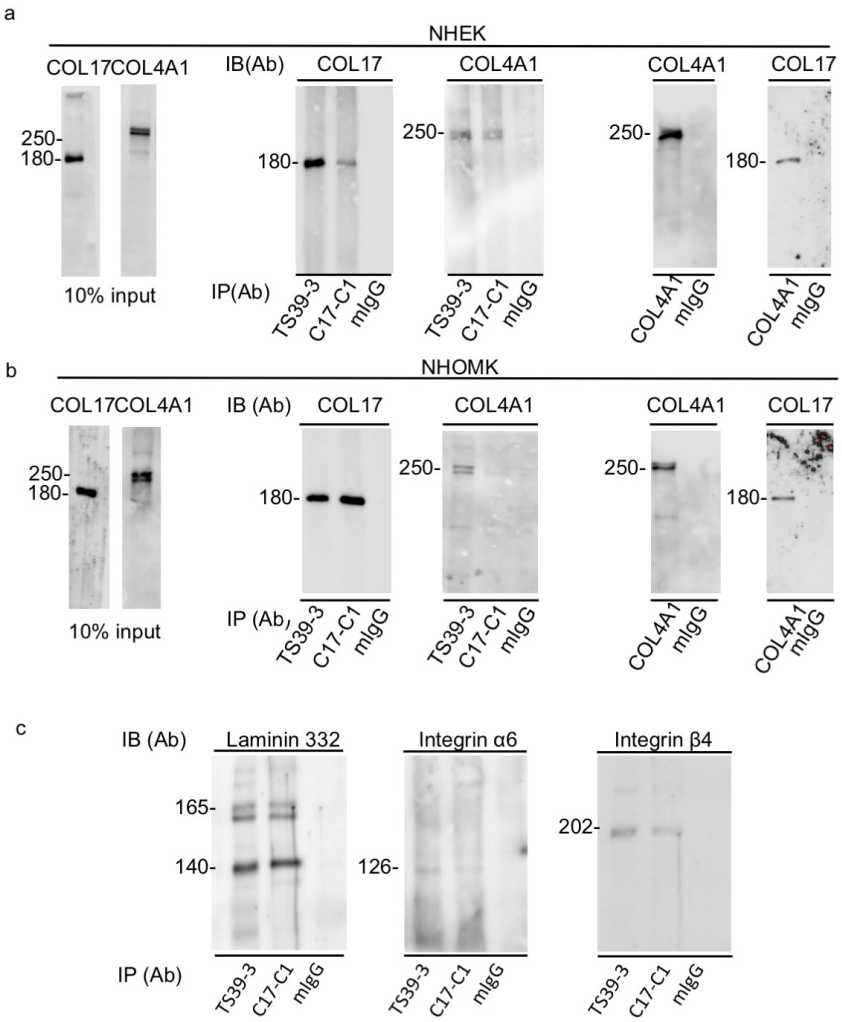

Figure 13 mAb targeting C-terminus (C17-C1) did not co-precipitate COL4

(a) Schema of full-length human COL17 and recombinant C-terminal-deleted COL17 (COL17Δ1, COL17Δ2) expressed by HEK293 cells. The epitopes of mAb TS39-3 (Asp^{552}-Gln^{545}) and mAb C17-C1 (Gly^{1316}-Asp^{1340}) are indicated. (b) Immunoprecipitation with mAbs TS39-3, C17-C1, anti-human COL4A1 Ab or mIgG1 using cell lysates of NHOMK. Blotting was performed using anti-human COL17 Ab or anti-human COL4A1 Ab. The protein amounts in the cell lysates were analyzed by immunoblotting as input (10% amount of IP). (c) Immunoprecipitation with mAbs TS39-3, C17-C1 or mIgG1 using cell lysates of NHOMK. Immunoblotting was performed using anti-human laminin 332, anti-human integrin α6 or anti-human integrin β4. IP (Ab): immunoprecipitation antibody, IB (Ab): immunoblotting antibody.

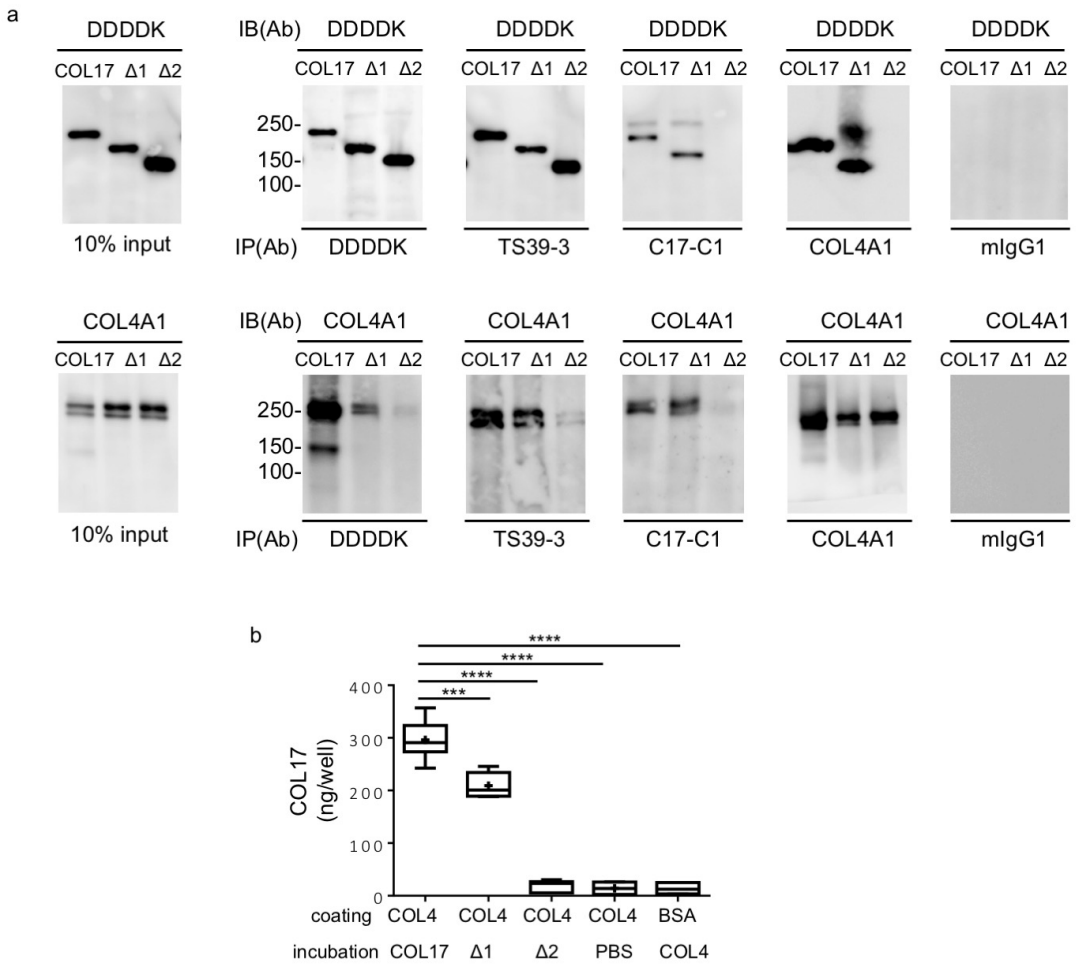

Figure 14 C-terminus of COL17 directly binds to COL4

(a) Immunoprecipitation with anti-DDDDK, mAbs TS39-3, C17-C1 or mIgG1 using cell lysates of HEK293 expressing recombinant human COL17 (full-length COL17, COL17Δ1, and COL17Δ2). Immunoblotting was performed using anti-DDDDK Ab or anti-human COL4 Ab. The protein amounts in the cell lysates were analyzed by immunoblotting as input (10% amount of IP). (b) *In vitro* binding test between COL17 and COL4. The plates were coated with human COL4 protein (500 ng/well) and then incubated with full-length COL17 (500 ng/well). To quantify COL17 binding amounts to COL4-coated plates, the standard curve was measured by serial diluted full-length human COL17. The data are expressed as the mean ± S.D. One-way ANOVA. ***0.0001<p<0.001, ****p<0.0001. IP (Ab): immunoprecipitation antibody, IB (Ab): immunoblotting antibody.

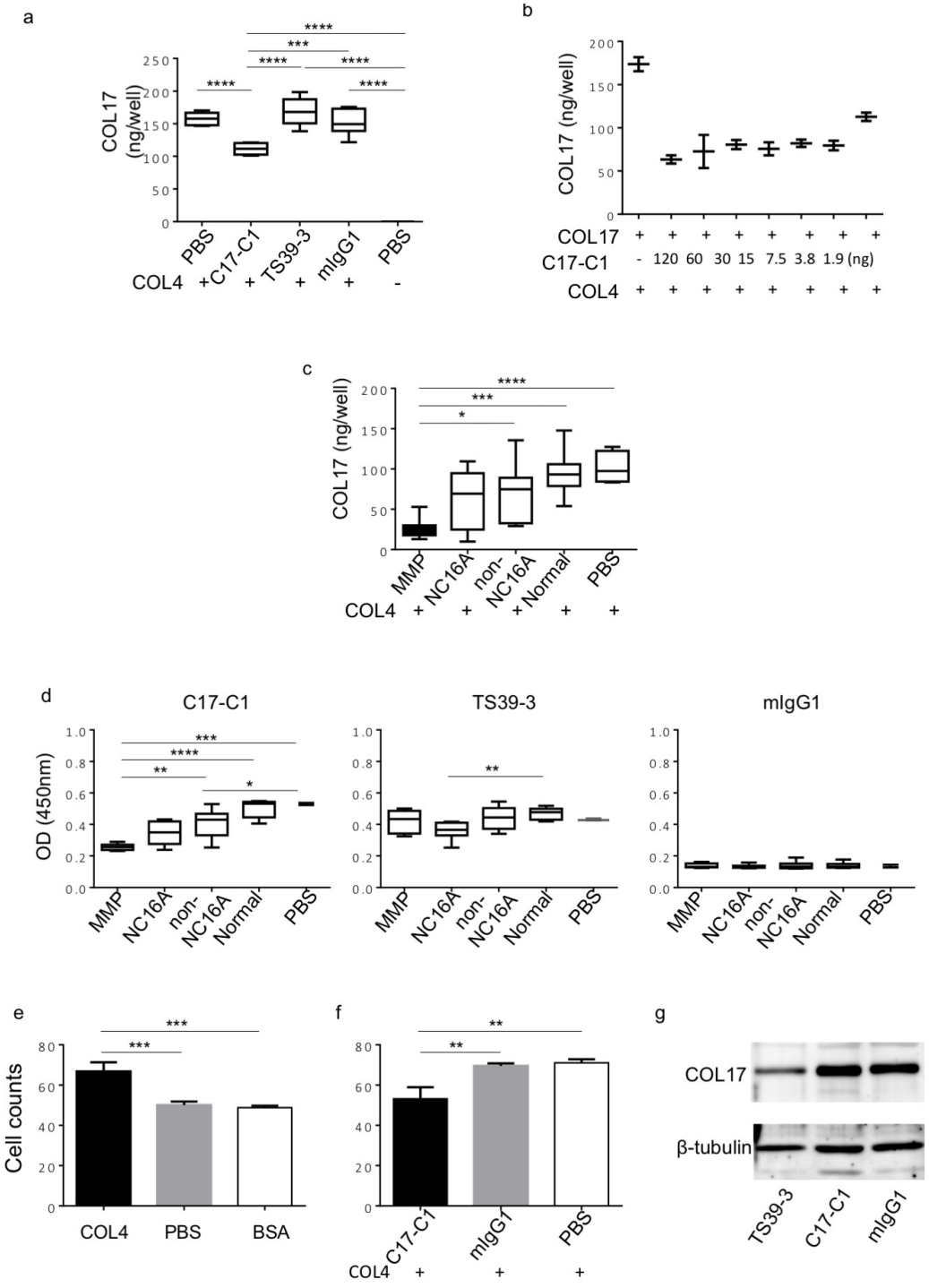

Figure 15 Autoantibodies targeting the C-terminus of COL17 disrupt the binding between COL17 and COL4

(a) *In vitro* binding inhibition test between COL17 and COL4 using mAbs against human COL17.The plates were coated with human COL4 proteins (500 ng/well).

Full-length human COL17 (250 ng/well) was preincubated with mAb C17-C1, mAb TS39-3, or mIgG1 (250 ng/well) and then added to the plates. To quantify COL17 binding amounts to COL4-coated plates, the standard curve was measured by serial diluted full-length human COL17. (b) *In vitro* inhibition test of the binding between COL17 and COL4 (250 ng/well) using serially diluted mAb C17-C1. To quantify COL17 binding amounts to COL4-coated plates, full-length human COL17 recombinant protein was used with serial dilutions.

(c) *In vitro* binding inhibition test between COL17 and COL4 using MMP-IgG, or BP-IgG. MMP-IgG, BP-IgG or normal human IgG (20 μg/well) was preincubated with full-length COL17 and then added to the COL4-coated plates (250 ng/well). To quantify COL17 binding amounts to COL4-coated plates, the standard curve was measured by serial diluted full-length human COL17. (d) Competitive COL17-ELISA using mAbs against human COL17 and MMP-IgG or BP-IgG. The full-length COL17-coated plates (250 ng/well) were incubated with MMP-IgG, BP-IgG, or normal human IgG, followed by the incubation with mAb C17-C1, mAbTS39-3, or mIgG1. (e) The remaining cell number in the culture plates with or without COL4 coating after vibration stress. (f)The remaining cell number in COL4-coated plates with the stimulation with mAb C17-C1 or mIgG1 after vibration stress (g) The relative COL17 amounts were evaluated after the 12-hour stimulation with mAbs C17-C1, TS39-3 or mIgG1. The data are expressed as the means ± S.D. One-way ANOVA. *$0.01<p<0.05$, **$0.001<p<0.01$, ***$0.0001<p<0.001$, ****$p<0.0001$.

	Forward primer (5'→3')	Reverse Primer (5' →3')
human		
hCOL7A1	5_-GGACGCGCAGGATGACG-3	5_-CAATGTCAGCGGCGTAAAGG-3
hCOL17A1	5_-TCAACCAGAGGACGGAGTCA-3	5_-TCGACTCCCCTTGAGCAAAC-3
hLAMC2	5_-ATCTGATGGACCAGCCTCTCA-3	5_-AGCCTGGGTATTGTAGCAGC-3
hITGA6	5_-CACTGCAGAGAGCCAACAGA-3	5_-TGACCCCCATCCACTGATCT-3
hITGB4	5_-GAGGGAGGAAGAGGATGGCA-3	5_-TCTTCACTGGGGCCTTCTTG-3
hKRT1	5_-TTGACAAGGTGAGGTTCCTGG-3	5_-TTGGTCCACTCTCCTTCGGA-3
hKRT4	5_-GGGCGAGGAGTACAGAATGT-3	5_-CCTAATCCTCCGCTGATGCC-3
hKRT13	5_-GGACGCCAAGAAGCGTCAG-3	5_-GGCGACCAGAGGCATTAGAG-3
hYWHAZ	5_-ACTTTTGGTACATTGTGGCTTCAA-3	5_-CCGCCAGGACAAACCAGTAT-3
mice		
mCol7a1	5_-CGGACTATGAGGTGACCGTG-3	5_-TGCTCAACAGAAGATGCGGT-3
mCol17a1	5_-GATGGCACTGAAGTCACCGA-3	5_-TATCCATTGCTGGTGCTCCC-3
mLamc2	5_-GGAGAGAACGGCTGTGTGTA-3	5_-CTGACTCAGTCCTGGCCCC-3
mItga6	5_-ATGCCACCTATCACAAGGCT-3	5_-GCATGGTATCGGGGAATGCT-3
mItgb4	5_-CCAGCACAACCACCGTTATTC-3	5_-TTGGCATTGGGGTTCTGTGG-3
mKrt1	5_-CAGTGTGGCCTGTCAATCAC-3	5_-GCTTCCAGAATCCAGGCTAGT-3
mKrt13	5_-CAGTGTGGCCTGTCAATCAC-3	5_-GCTTCCAGAATCCAGGCTAGT-3
mGapdh	5_-AACATCAAATGGGGTGAGGCC-3	5_-GTTGTCATGGATGACCTTGGC-3

Table 1 Primer sequence

MMP Case	Age	Sex	Skin	Oral mucosa	DIF[a]	ssIIF[b]	ELISA[c]	HE[d]	Immunoblotting		Type[e]	Normal human IIF						Immmunoblotting		Autoantigen[h]
												IgG				IgA				
									Epidermal	Dermal		S1[f]	S2[f]	M1[g]	M2[g]	S[f]	M[g]	NHEK	NHOMK	
1	75	M	-	+	G,C3	E	32	+	-	-	COL17	-	-	-	-	-	-	-	180kDa	COL17
2	60	F	+	+	C3	E	53.5	+	180kDa	-	COL17	-	20	20	80	-	-	-	180kDa	COL17
3	62	F	-	+	n.d	E	76.9	n.d	180kDa	-	COL17	-	10	40	40	-	-	-	180kDa	COL17
4	53	F	-	+	G,C3	E	18.3	+	-	200KDa	COL17	-	-	10	10	-	-	-	-	undetected
5	81	F	-	+	G	E,D	9.4	-	-	-	unknown	-	-	-	10	-	-	-	180kDa	COL17
6	66	F	+	+	G,C3	-	160	-	180kDa	-	COL17	20	40	20	80	-	-	-	180kDa	COL17
7	39	F	+	+	G,C3	E	-	n.d	-	-	unknown	-	-	10	-	-	-	-	-	undetected
8	65	F	-	+	G	-	-	+	-	-	unknown	-	10	10	40	-	-	-	180kDa	COL17
9	83	F	-	+	G,A	E	-	+	-	-	unknown	-	-	10	10	-	-	-	-	undetected
10	82	M	+	+	G,A,C3	E	13.9	+	180kDa	-	COL17	10	10	20	40	-	-	-	180kDa	COL17
11	72	F	+	+	G,C3	E	-	+	-	-	COL17	10	10	10	20	-	-	-	180kDa	COL17
12	81	F	-	+	G,A	-	-	-	-	-	unknown	-	-	-	-	-	-	-	-	undetected
13	72	F	-	+	G,A,M,C3	E	-	-	-	-	unknown	-	-	-	-	-	-	-	-	undetected
14	67	F	-	+	G,A,C3	-	-	+	-	-	unknown	-	-	-	10	-	2	-	-	undetected
15	73	M	+	+	G	E	-	+	-	-	unknown	20	40	20	80	-	-	180kDa	180kDa	COL17
16	79	F	-	+	G,C3	-	-	-	-	-	unknown	-	-	10	40	-	-	-	-	undetected
17	76	M	+	+	G,C3	D	-	+	-	-	unknown	-	-	-	20	-	-	140kDa	140kDa	Laminin332
18	66	M	+	+	G,C3	D	-	-	-	-	unknown	-	-	-	20	-	-	-	-	undetected
19	52	F	-	+	G,C3	-	-	n.d	-	-	unknown	-	-	10	20	-	-	-	180kDa	COL17
20	78	M	-	+	G,C3	-	-	n.d	-	-	unknown	-	-	-	10	-	-	-	-	undetected
	total		40%	100%	100%	65%	35%	63%	20%	5%	35%	35%		85%		0%	5%	10%	55%	55%
													*						*	

BP Case	Age	Sex	Skin	Oral mucosa	DIF	ssIIF[b]	ELISA[c]	HE[d]	Type[e]	S1[f]	S2[f]	M1[g]	M2[g]	NHEK	NHOMK
1	60	M	+	-	C3	E	1282	+	COL17	320	320	320	320	180kDa	180kDa
2	79	M	+	-	G,C3	E	63	+	COL17	320	320	160	160	180kDa	180kDa
3	44	F	+	-	G,C3	E	2240	+	COL17	320	320	320	320	180kDa	180kDa
4	61	F	+	-	G	E	294	n.d	COL17	80	80	40	40	180kDa	180kDa
5	72	M	+	+	G,C3	E	106	n.d	COL17	320	320	320	320	180kDa	180kDa
6	75	M	+	+	G,C3	E	44.7	+	COL17	40	80	40	40	180kDa	180kDa
7	50	M	+	-	G,C3	E	746	+	COL17	80	160	80	80	180kDa	180kDa
8	82	M	+	-	G,C3	E	196	+	COL17	160	160	160	160	180kDa	180kDa
9	60	M	+	-	G,C3	E	682	+	COL17	320	320	320	320	180kDa	180kDa
10	87	F	+	-	G,C3	E	43.9	+	COL17	40	80	80	80	180kDa	180kDa
11	78	M	+	+	G,C3	E	53	n.d	COL17	80	160	80	40	180kDa	180kDa
12	58	F	+	-	C3	E	306	+	COL17	160	320	80	160	180kDa	180kDa
13	77	M	+	-	G,C3	E	28	n.d	COL17	40	80	40	40	180kDa	180kDa
14	81	M	+	-	G,C3	E	150	+	COL17	320	320	320	320	180kDa	180kDa
15	71	F	+	-	G,C3	E	25.3	+	COL17	40	40	20	20	180kDa	180kDa
16	79	M	+	-	G,C3	E	53.3	+	COL17	160	320	160	160	180kDa	180kDa
17	49	F	+	-	G,C3	E	202	+	COL17	320	320	320	320	180kDa	180kDa
18	76	M	+	-	G,M,C3	E	41.9	+	COL17	40	40	-	-	180kDa	180kDa
19	75	F	+	-	G,C3	E	202	+	COL17	320	320	320	320	180kDa	180kDa
20	92	F	+	-	G	E	16.5	+	COL17	20	20	20	20	-	-
	total		100%	15%	100%	100%	100%	80%	100%	100%		95%		95%	95%

Table 2 The results for 20 cases of MMP and 20 cases of BP patients.

a: DIF was not performed for MMP case 3. b: 1M NaCl-split skin IIF. c: COL17NC16A ELISA. d: Hematoxylin and eosin stain. e: MMP or BP type determined by conventional laboratory examinations including COL17-NC16A ELISA and immunoblotting. f: Skin. g: Mucosa. h: The autoantigen identified in this study. E: Epidermal side. D: Dermal side. G: IgG. A: IgA. Student's *t*-test. *0.01<p<0.05

	MMP (n=20)	BP (n=20)
IIF (normal human)		
Skin	7 (35%)	20 (100%)
Oral mucosa	17 (85%)	18 (90%)
IIF (COL17 humanized mouse)		
Skin	7 (35%)	20 (100%)
Bbuccal mucosa	10 (50%)	20 (100%)
Tounge	4 (25%)	20 (100%)
Esophagus	8 (40%)	20 (100%)
Immunoblotting		
NHEK lysate	2 10%)	19 (95%)
NHOMK lysate	11 (55%)	19 (95%)

Table 3 The overall results for the MMP and BP patients.

Student's *t*-test. *0.01<p<0.05

BP case	DIF	IIF	ssIIF	ELISA
1	G, C3	80	E	340
2	G, C3	80	E	300
3	G, C3	320	E	336
4	G, C3	80	E	238
5	G, C3	320	E	18.9
6	G, C3	80	E	354

MMP case	DIF	IIF	ssIIF	ELISA
1	G, A, C3	-	E	-
2	G, C3	80	E	70
3	G, C3	20	E	-
4	G, A, C3	80	E	32
5	G, C3	80	E	-
6	G, A, C3	-	E	35.8
7	G, A	-	E	13

Table 4 The laboratory data of BP cases (n=6) and MMP cases (n=7). For the diagnosis, the following tests were performed: direct immunofluorescence (DIF), indirect immunofluorescence (IIF), 1M NaCl normal human split skin IIF (ssIIF) (sera dilutions; 1:10), and ELISA. DIF results show the deposition antibody-isotype and complement at the basement membrane zone (G: IgG, A: IgA, C3: complement C3). The deposits in DIF and IIF were observed along the basement membrane zone (BMZ). IIF results show the titer of IgG autoantibodies determined by serial dilution. ssIIF shows IgG deposits on the epidermal side of the lamina lucida (E). ELISA results show the index of COL17-NC16A ELISA.

MMP-IgG			NC16A BP-IgG			non-NC16A BP-IgG			normal IgG		
IIF	ssIIF	ELISA	IIF	ssIIF	ELISA	IIF	ssIIF	ELISA	IIF	ssIIF	ELISA
80	E	51.8	320	E	117.7	160	E	294.0	-	-	4.1
80	E	1.5	320	E	123.5	80	E	3.3	-	-	2.0
80	E	1.4	160	E	73.7	80	E	1.4	-	-	5.5
						80	E	5.0			

Table 5 IIF titer, 1M NaCl normal human split skin IIF (ssIIF) (1:10), and COL17-NC16A ELISA index of purified MMP-IgG, BP-IgG, and normal IgG (20 mg/ml). E: epidermal side.